Available online at www.sciencedirect.com

ScienceDirect

Current Opinion in
Colloid & Interface Science

Emerging strategies for the formulation of antibody–nanoparticle conjugation in lateral flow immunoassays

Helena Mateos[1] and Miquel Oliver[2,3]

Lateral flow immunoassays (LFIAs) are indispensable point-of-care diagnostic tools due to their simplicity, fast readout and low cost. Traditionally based on gold nanoparticles (AuNPs) for visual detection, recent advances in nanotechnology have expanded the LFIA toolkit to include a wide range of nanoparticles (NPs), such as carbon NPs, quantum dots, upconversion NPs, nanozymes, aggregation-induced emission nanoparticles, and bimetallic or hybrid structures. These novel nanomaterials improve assay sensitivity and allow for multimodal detection (using fluorescence, surface-enhanced Raman scattering or photothermal detection). Central to the performance of NP-based LFIAs is the protein corona, typically formed by antibodies, which mediates antigen recognition. Immobilization strategies range from simple physisorption to more controlled chemisorption techniques (e.g., 1-ethyl-3-(3-dimethylaminopropyl) carbodiimide/N-hydroxysuccinimide carbodiimide coupling, thiol- or glycan-directed attachment) and bioaffinity methods (e.g., biotin–streptavidin). Although chemisorption is often assumed superior, a critical comparison of recent studies reveals that optimized physisorption can achieve similar or better detection limits in many cases. Conjugation strategy, NP morphology, and surface chemistry collectively influence probe stability, orientation, and binding efficiency. This review critically evaluates recent innovations in nanoparticle selection, conjugation methods, and signal generation strategies.

Addresses
[1] Chemistry Department, University of Bari Aldo Moro, Via Orabona, 4, 70126, Bari, Italy
[2] FI-TRACE Group, Department of Chemistry, University of the Balearic Islands, Carretera de Valldemossa km 7.5, E-07122, Palma de Mallorca, Spain
[3] CNR-IFN (National Research Council – Institute for Photonics and Nanotechnologies), c/o Physics Department, University of Bari, Via Amendola 173, 70126, Bari, Italy

Corresponding author: Mateos, Helena (helena.mateos@uniba.it)

Current Opinion in Colloid & Interface Science 2025, **80**:101968

This review comes from a themed issue on **Formulation and Cosmetics**

Edited by **Samiul Amin** and **Gerardo Palazzo**

For a complete overview see the Issue and the Editorial

https://doi.org/10.1016/j.cocis.2025.101968

Introduction

Lateral flow immunoassays (LFIAs), especially after COVID19 pandemic, have established themselves as indispensable diagnostic tools due to their simplicity, low cost, rapid analysis times, and minimal instrumentation requirements [1–5]. From point-of-care testing in clinical diagnostics to food safety monitoring and environmental analysis, LFIA platforms are widely used for the qualitative and semiquantitative detection of a broad range of analytes [1,2,6–9].

In a typical LFIA, the sample is applied onto a sample pad and migrates by capillary action along a porous nitrocellulose membrane. First, the analyte binds to detection antibodies that have been conjugated to nanoparticles, forming an analyte–antibody–nanoparticle complex in the conjugate pad. This complex continues to migrate and is captured by immobilized capture antibodies at the test line, producing a visible signal. Excess conjugate binds at the control line to confirm proper assay function. The final result is typically interpreted by the appearance (or absence) of colored lines, allowing for rapid visual readout without the need for specialized equipment (Figure 1) [1,10,11].

Traditionally, assay performance has relied on gold nanoparticles (AuNPs) as visual labels owing to their distinctive optical properties arising from localized surface plasmon resonance (LSPR). The collective oscillation of conduction band electrons upon interaction with visible light produces their characteristic intense red color of the test and control lines [12–14]. However, the inherent limitations of conventional LFIA, particularly in terms of sensitivity, quantitative accuracy, and multiplexing capability, have driven significant research efforts toward the development of advanced nanoparticle-based probes and alternative detection strategies [6,15–22].

In recent years, nanotechnology has been revolutionizing LFIA design. Diverse nanoparticles including selenium, carbon, quantum dots (QDs), upconversion nanoparticles (UCNPs), nanozymes, and bimetallic or hybrid nanostructures have been explored to overcome the sensitivity limitations of traditional colorimetric

Figure 1

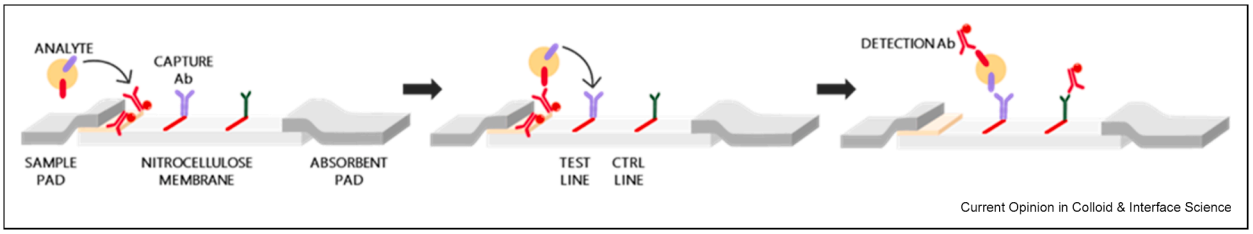

Schematic of a typical sandwich lateral flow immunoassay (LFIA) format. The sample (left) is applied to the sample pad and migrates by capillarity, carrying target analytes (red) that bind to nanoparticle-labeled detection antibodies (red). This complex continues to migrate and is captured by immobilized capture antibodies (purple) at the test line, producing a visible signal. Excess conjugates are captured at the control line by secondary antibodies (black).

systems [4,15,16,22–26]. Each nanoparticle type offers unique physicochemical properties that influence its optical behavior, surface reactivity, and interaction with biological recognition agents. This evolution has been accompanied by the integration of multimodal detection approaches such as fluorescence, surface-enhanced Raman scattering (SERS), photothermal, electrochemical, and magnetic readouts, further expanding the capabilities of LFIA beyond binary visual outputs [5–8,16,27–32].

Central to the successful implementation of nanoparticle-based LFIAs is the protein corona, the layer of biomolecules (primarily antibodies) adsorbed or covalently bound to the nanoparticle surface. The structure, orientation, and stability of this protein layer directly impact antigen recognition, assay sensitivity, and reproducibility [13,33–40]. While physisorption remains the most straightforward and widely used conjugation method due to its simplicity and ability to preserve antibody functionality, its random antibody orientation and weak binding can compromise assay performance, particularly under complex sample conditions. Conversely, chemisorption strategies including amine-based covalent coupling, sulfhydryl-directed immobilization, carbohydrate-specific attachment, and bioaffinity-based biotin–streptavidin interactions provide stronger, more controlled conjugation, but they often require additional chemical modifications, increasing cost and preparation time [3,13,16,18,28,33,34,41–46].

The design of LFIA nanoprobes thus requires a delicate balance among nanoparticle selection, conjugation chemistry, and detection modality, each tailored to the specific analytical target and operational context. Moreover, emerging trends demonstrate a shift toward multifunctional hybrid systems capable of simultaneous target enrichment, capture, and multimodal detection. These systems often integrate magnetic cores for sample clean up and/or preconcentration [9,27,47–49] and plasmonic or fluorescent layers for enhanced readouts [21,25,50–52]. Although sustainability is increasingly recognized as a priority in nanotechnology, explicit efforts within LFIA research remain limited. Most recent advances have concentrated on improving sensitivity and multiplexing, with only a few examples touching on sustainability, for instance, the replacement of animal-derived antibodies with recombinant biorecognition elements such as nanobodies or affibodies [35,46,53,54]. This gap underscores an opportunity for future LFIA development to adopt greener nanoparticle synthesis routes and more sustainable biorecognition strategies [22].

This review aims to provide an updated and critical overview of nanoparticle types used in LFIA, focusing on their interactions with protein corona, and immobilization strategies, highlighting recent innovations and current challenges. We discuss the physicochemical characteristics of each nanoparticle class, their advantages and limitations in LFIA applications, the role of protein corona in determining assay performance, and the chemistries employed to achieve stable and functional bioconjugation.

Nanoparticle types and their interaction with protein corona

Nanoparticles are central to the function and performance of LFIA, acting as carriers, signal generators, and platforms for biorecognition. This section provides an overview of the main types of nanoparticles used in LFIA, including colored, fluorescent, magnetic, and hybrid systems, and how their structural and surface properties influence assay sensitivity, stability, and multiplexing capability. A key focus is the interaction between nanoparticles and antibodies, which leads to the formation of a protein corona that can affect bioactivity, orientation, and binding efficiency. Strategies for

controlling or engineering this corona, such as covalent coupling or affinity-based conjugation, are discussed alongside the impact of surface chemistry. Additionally, advanced detection mechanisms such as Raman, photothermal, and electrochemical readouts are reviewed, highlighting how nanoparticle design enables enhanced signal output and assay performance in increasingly complex sample matrices. Table 1 provides a series of current examples on these concepts.

Colored or visual nanoparticles

Colored nanoparticles remain the most widely used labels in lateral flow immunoassays due to their intense optical properties, ease of synthesis, and compatibility with naked-eye detection. While AuNPs are the traditional choice, alternative nanoparticle labels such as selenium, platinum (Pt), carbon, and latex have also been employed to expand color options, improve stability, and enhance signal intensity. These visually detectable probes form the backbone of traditional LFIA formats, offering simplicity, low cost, and robust performance for point-of-care diagnostics.

Gold nanoparticles and other metallic colored nanoparticles

Gold nanoparticles have long been used in bioassays due to their intense red color. Since the work by Michael Faraday in 1850, many chemical and physical techniques have been developed and improved for the synthesis of AuNPs in various shapes and sizes [12]. Recent studies show both continuity and innovation in AuNP-based LFIA. Traditional spherical AuNPs remain widely used for their simplicity and reliable plasmonic colorimetric signal as in the works by Jia et al. for dichlorvos (16–108 μg/kg) [14], Díaz-Avello et al. for tetrodotoxin (0.3 ng/mL) [55], and Prakashan et al. for SARS-CoV-2 detection [1], confirming their robustness in food safety and clinical diagnostics. These works reaffirm that with optimized conjugation and proper assay design, classical AuNPs still yield excellent performance without needing advanced nanoparticle structures. However, emerging trends include the use of engineered AuNP morphologies such as nanostars as shown by Liu et al. [56], where gold nanostars enabled dual-mode colorimetric, photothermal detection of carbendazim in the range of 0.28–0.48 ng/mL, exploiting their branched morphology for enhanced near-infrared (NIR) absorption. In parallel with advances in nanoparticle design, novel recognition strategies are also emerging as Sadler et al. demonstrated with affibodies (see Figure 2), small (7 kDa compared to 150 kDa for antibodies), robust (able to withstand extreme temperatures (up to 95 °C) and pH (3–11)), and easily engineered protein ligands as stable and scalable alternatives to conventional antibodies. Moreover, their structure lacks animal-derived Fc regions, which reduces cross-reactivity issues. By leveraging His-tag-mediated adsorption onto AuNPs, these mimetic antibodies achieved effective conjugation while maintaining high target specificity and signal stability, suggesting a promising route for next-generation LFIA probes [53].

Although AuNPs are the most widely used and studied nanoparticles in LFIA, there are others that have been also employed as colorimetric probes, despite the lack of LSPR, such as selenium or Pt nanoparticles.

Selenium NPs have been used as a cheaper and more stable alternative to AuNPs [4], being insensitive to salt ions-induced aggregation and hence suitable for labeling proteins that can be dissolved in high-salt environments. SeNPs exhibit an orange color regardless of the capping agent thus allowing naked-eye detection. For example, in the work performed by Wang et al., SeNPs have been used in dual-target assay for the simultaneous quantification of anti-SARS-CoV-2 IgG and IgM using 2 test lines on the same strip [57]. In blood samples, hemolysis proved to be a problem as it altered the intensity of the test line leading to inconsistent analyte quantification [58].

Although some studies have been performed using Pt NPs for visual detection [23], Pt is more commonly employed together with other metal in core-shell format or as nanozymes due to its peroxidase-like activity as it will be discussed in the next sections.

Other kinds of NPs used in colorimetric detection

Polymer-based nanoparticles, which allow the color to be selected simply by the incorporation of different dyes or carbon and magnetic nanoparticles among others, which have also gained interest due to their strong intrinsic color and multifunctional properties providing flexibility in assay design.

Carbon NPs (CNPs) represent a cost-effective alternative to gold that can be easily visualized by the naked eye. Mussin et al. [24] used avidin-CNPs which were fixed in the conjugated pad and interacted with DNA prepared in a previous step through a double-tagging PCR using biotin and digoxigenin for fungal *Paracoccidioides* pathogen recognition. The use of a smartphone and portable thermocycler for the PCR step allows this system for point-of-care applications. Bismuth sulfide nanoparticles (Bi_2S_3 NPs) show a dark brown color and have been recently used as a colorimetric probe taking also advantage of the intrinsic

Table 1

Selected recent examples of LFIAs (2023–2025) showing how conjugation strategy, nanoparticle type, and label architecture impact analytical performance.

Ref	Year	NP used	Conjugation strategy	Conjugated biomarker	Analyte	LOD	Detection/readout type
[1]	2023	AuNPs	Physisorption	Receptor-binding domain antibody	SARS-CoV-2 RBD antigen	0.30 ng/mL	Colorimetric/smartphone
[53]	2025	Catalytic PtNPs and AuNPs	Physisorption with hexahistadine (His_6) tag	Helical affibodies dimers	SARS-CoV-2 spike (S) protein	6 pM	Colorimetric
[4]	2025	PEG-SeNPs	Electrostatic adsorption	Protein probes	SARS-CoV-2 antigen	0.01 ng/mL	Colorimetric/smartphone
[24]	2024	Av-CNPs	Physisorption and avidin-biotin	Bioting/digoxigenin double-tagged amplicon	*Paracoccidioides* spp. DNA amplicons	0.1 ng	Colorimetric/smartphone
[60]	2025	Latex microspheres (LMs)	EDC/NHS chemistry	Cryptococcus capture antibody	Cryptococcus	3000 CFU/mL	Colorimetric/smartphone
[89]	2023	Fe–N–C single-atom nanozyme	Physisorption	Anti-FB_1 and AFB_1 mAbs	Mycotoxins AFB_1 and fumonisom B_1 (FB_1)	0.0028 ng/mL and 0.013 ng/mL for AFB_1 and FB_1	Colorimetric/smartphone
[7]	2024	EuNPs	EDC/NHS chemistry	Anti-nitrofuran mAb	Nitrofuran antibiotics	0.013, 0.019 and 0.023 ng/mL for AOZ, AMOZ and NFS	Fluorescence
[31]	2024	Kiwi-type magneto-fluorescent silica nanohybrid (MFS)	EDC/NHS chemistry	Anti-cTnI mAb	Cardiac troponin I (cTnI)	0.0084 ng/mL	Fluorescence
[41]	2025	AIEgens packed into DMSNs	Physisorption	Anti-T2 and anti–*Staphylococcus aureus* enterotoxin A (SEA) antibody	T2 toxin and SEA)	0.2 and 0.43 ng/mL for T2 and SEA in fluorescence	Dual (colorimetric–fluorescent)
[25]	2023	Au–Ag hollow nanoshells (Au–Ag HNSs)	EDC/NHS chemistry	SARS-CoV-2 S protein	SARS-CoV-2 neutralizing antibody	20 ng/mL	Tri-mode (Colorimetric, photothermal, and SERS)
[22]	2024	Flower CuO@Ag NPs	Not specified	Not specified	Clenbuterol hydrochloride (CLE)	0.6 ng/mL and 8 ng/mL	Colorimetric/photothermal
[68]	2024	DMSNs/AuNPs@Ag	Physisorption	Second anti-AFP mAb	α-fetoprotein (AFP)	0.85 ng/mL	Electrochemical
[74]	2023	La^{3+}-doped UCNPs	EDC/NHS chemistry	ZEN mAb	ZEN	0.25 ng/mL	Fluorescence
[80]	2024	AuNPs	Sulfhydryl-based strategy	Aptamer MSA52	SARS-CoV-2 S proteins	91.2 ng/mL	Colorimetric
[55]	2025	AuNPs	Au–S bonding	Aptamer	Tetrodotoxin	8 ng/mL	Colorimetric
[45]	2025	AuNPS	Biotin/avidin-free sandwich aptamer-based assay	Aptamer	*Trichomonas vaginalis*	1.6×10^5 cell/mL	Colorimetric
[37]	2025	EuNP	Fc-specific peptide for oriented antibody immobilization	AFB1 antibody	AFB1	0.05 ng/mL	Fluorescence
[86]	2025	AuNPs	Biotin/streptavidin	Anti-immunocomplex peptides (AIcPs)	Deltamethrin	6.25 ng/mL	Colorimetric
[46]	2025	AuNPs	Biotin/streptavidin	Nanobody	*Salmonella typhimurium*	10^3 CFU/mL	Colorimetric
[87]	2025	SA@AuNPs	Biotin/streptavidin	Sulfo–NHS–biotin labeling lipoprotein of bacterial surface.	Pathogenic bacteria	1×10^4 to 5×10^4 CFU/mL	Colorimetric
[35]	2023	SA@QDs	Nanobody-oriented coupling strategy biotin/streptavidin	Nanobody-Avi tag	AFB1	0.095 ng/mL	Fluorescence
[90]	2025		Electrostatic adsorption	Rabbit anti-human IgG antibody	Human immunoglobulin G (H-IgG)	0.269 ng/mL	Colorimetric

		(Metal-organic framework) MOF@PtNi nanocomposite				
[49]	2024	Magnetic nanocomposite (Fe_3O_4@PEI/Au^{MBA}@Ag-MBA)	EDC/NHS chemistry	AFB1-mAb and ZEN-mAb	AFB1 and ZEN	0.095 ng/mL and 0.00476 ng/mL for ZEN and AFB1 SERS

AFB1, aflatoxin B1; AuNPs, gold nanoparticles; EDC/NHS, 1-ethyl-3-(3-dimethylaminopropyl) carbodiimide/N-hydroxysuccinimide; LOD, limit of detection; mAb, monoclonal antibody; MBA, 4-mercaptobenzoic acid; Pt, platinum; QD, quantum dot; RBD, receptor-binding domain; SERS, surface-enhanced Raman scattering; UCNPs, upconversion nanoparticles; ZEN, zearalenone.

hydrogen bonding that enables the covalent conjugation with monoclonal antibodies (mAbs) [59] enhancing stability and the number of attached antibodies over time.

Latex nanoparticles are among the most commonly used colorimetric nanoprobes as they are commercially available in various sizes, colors, and prefunctionalized forms. Chen et al. [2] used 200 nm carboxylated latex microspheres in three different colors, which were conjugated with different mAbs through 1-ethyl-3-(3-dimethylaminopropyl) carbodiimide (EDC), in combination with N-hydroxysuccinimide (NHS), enabling the simultaneous detection of multiple mycotoxins in cereals. Recently Zang et al. developed an LFIA for the detection of the pathogenic fungus Cryptococus in the serum using red latex microspheres that were conjugated via EDC/NHS with the appropriate mAb [60]. The immunoassay achieved a limit of detection (LOD) of 3000 CFU/mL, eight times lower than using AuNPs. Although polymeric NPs can be used alone for colorimetric detections, in many cases, they are employed as carriers to encapsulate and stabilize other NPs as demonstrated in some of the following examples.

Regarding colored NPs, in another study, polydopamine (PDA)-coated and dye-loaded cellulose nanoparticles (dCNPs@P) were used in different colors [61]. PDA was utilized to keep the dye encapsulated, stabilize the colloidal suspension over a broad pH and NaCl concentration range and provide a reactive surface for protein corona formation via Michael addition and Schiff base reactions. The NPs, loaded with different dyes, were conjugated with various mAbs, enabling the simultaneous detection of up to three different inflammatory biomarkers with LODs slightly lower than those obtained using traditional AuNPs.

Nanozymes are nanomaterials that exhibit enzyme-mimicking catalytic activities, such as peroxidase-like or oxidase-like reactions, increasingly used as catalytic labels in LFIA. They offer high stability, low cost, and tunable activity compared to natural enzymes; however, they lack substrate-specific active sites, limiting selectivity. To overcome this, bioreceptors such as antibodies, aptamers, or oligonucleotide probes are attached to nanozyme surfaces, forming a selective protein corona. Additionally, molecularly imprinted polymers (MIPs) can be applied to nanozyme surfaces to provide artificial antibody-like recognition via lock-and-key binding [62]. Nanozymes are composed of metals (e.g. gold, Pt, copper), metal oxides (e.g. cerium oxide, Fe_3O_4), carbon-based nanomaterials, or nanocomposites integrating multiple catalytic functionalities. Recent studies illustrate their practical potential in LFIA. For example, Pt nanozymes catalyzed 3,3′,5,5′-tetramethylbenzidine oxidation, lowering chlorpyrifos detection limits by up to 100-fold versus AuNP-based assays [63] while Fe_3O_4

Figure 2

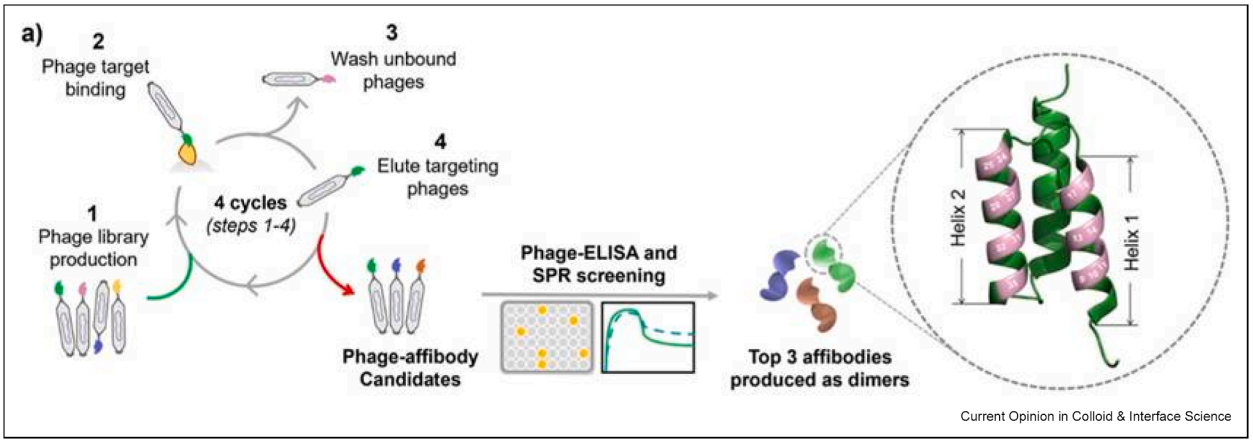

Schematic representation of the phage display process used to identify affibody candidates against the SARS-CoV-2 receptor-binding domain (RBD) or S1 protein (check Ref. [53] for a deeper understanding). Following iterative biopanning cycles, candidate binders were screened for specificity and affinity. The structural model highlights the characteristic three-helix bundle fold of affibody molecules (image generated with PyMOL, Schrödinger).

nanozymes provide peroxidase-like activity with magnetic separation [64].

These approaches consistently demonstrate three main advantages. First, nanozymes improve assay sensitivity through catalytic amplification as their enzymatic activity generates intense detectable signals even at low analyte concentrations, significantly lowering the limit of detection compared to conventional colorimetric probes. Second, they enable the detection of analytes that are otherwise challenging to quantify due to weak direct signals or low abundance, thereby broadening the applicability of LFIA platforms. Third, the intrinsic multifunctionality of many nanozymes, such as the magnetic properties of Fe_3O_4-based systems or hybrid metal oxide composites, allows integration of sample preconcentration, catalytic signal generation, and alternative detection modes within a single assay format.

Fluorescent NPs

Fluorescence-based LFIA offers improved sensitivity and quantification compared to colorimetric methods. Unlike AuNPs, which rely on visual signals, fluorescent nanoparticles emit light upon excitation, enabling lower LODs and more precise quantification.

Over the past five years, the use of europium nanoparticles (EuNPs) in LFIAs have gained attention due to their strong fluorescence, long emission lifetime, and high signal-to-noise ratio. Unlike traditional AuNPs, the lanthanide Eu offers intense, long-lived fluorescence with large Stokes shifts, resulting in low background interference from the nitrocellulose membrane. Jin et al. [6] and Mei et al. [7] demonstrated multiplex detection using carboxylated EuNPs and multiline strip formats to simultaneously identify five bacterial pathogens and three nitrofuran metabolites, respectively. Liang et al. [5] advanced the approach further using Eu(III)-chelate-doped polystyrene microspheres and time-resolved fluorescence to detect multiple mycotoxins while minimizing background and crosstalk. Fu et al. [8] extended the use of EuNP-LFIA into environmental health, developing a sensitive and stable assay for a urinary benzene metabolite, S-phenyl mercapturic acid (S-PMA) suitable for population-level smoke exposure monitoring.

Quantum dots (QDs) are semiconductor nanocrystals known for their high quantum yield (QY) and broad excitation/narrow emission spectra, enabling multiplex detection and usually providing higher sensitivity than the common LFIA based in AuNPs. The use of shells coating the core of QDs improves stability, reduces their toxicity, and increases the QY compared to traditional QDs as proved in recent studies. Current advances reveal a trend toward multifunctional nanostructures designed to overcome sensitivity limitations of traditional systems. One strategy involves brightness enhancement through structural engineering, as demonstrated by Li et al. [30], who created silica core-dual QD-shell nanocomposites (SI/DQD) containing two dense QD layers, enabling simultaneous methamphetamine and tramadol detection at sub-ng/mL levels using a handheld reader. Another emerging approach combined magnetic enrichment with fluorescent amplification, exemplified by Li et al. [31] who designed kiwi-inspired magneto-fluorescent silica nanohybrids embedding Fe_3O_4 cores within QD-loaded dendritic silica, achieving pg/mL-level cardiac troponin I detection with magnetic separation to reduce

background noise. Additionally, quenching-based amplification strategies are gaining attention. Jiang et al. [65] developed an inner filter effect-based competitive LFIA for mycotoxins where flower-like AuNPs quenched red-emitting QDs, generating a turn on signal that increased with analyte concentration. Similarly, Ding et al. [15] employed a nanometal surface energy transfer-based LFIA using QD microspheres as donors and AuNPs as acceptors to achieve 10-fold sensitivity improvement for T2 toxin detection.

Upconversion nanoparticles are a promising alternative for fluorescence-based LFIA due to their ability to convert NIR light into visible emission via multiphoton absorption. Typically composed of rare-earth-doped materials (e.g., $NaYF_4$: Yb^{3+}, Er^{3+}, Tm^{3+}), UCNPs offer several advantages, including low background noise due to the anti-Stokes phenomenon that blocks all the naturally occurring fluorescence, as well as high photostability, and narrow emission peaks. These properties provide a clear advantage over QDs and organic dyes, which suffer from autofluorescence and photobleaching. The integration of UCNPs into LFIA enhances detection sensitivity, allowing for improved quantitative and multiplex assays. [16,17]. In one study [32], polyacrylic acid was used to stabilize the UCNPs improving their dispersion in water with negligible impact on the emission intensity. The system was applied for the detection of the antibacterial agent olaquindox in food matrixes. For antibody conjugation, covalent coupling via the active ester method using EDC/NHS remains the standard approach for fluorescent nanoparticles. These studies reflect common trends: enhancing sensitivity via quenching-based amplification, achieving multiplexing through spectral separation, and integrating portable fluorescence readers for field deployment. However, despite their unique anti-Stokes emission and low background noise, UCNPs generally exhibit lower quantum yields than QDs or EuNPs and require near-infrared excitation sources, making the required instrumentation more complex and potentially limiting their widespread adoption in this field.

One of the most challenging issues with fluorophores is their aggregation at high concentrations, which leads to a decrease in their emission due to self-quenching. Aggregation-induced emission luminogens (AIEgens), with aggregation-induced emission, counteract this drawback [18,66]. Typically, to promote the aggregation of these molecules, a matrix is used to encapsulate the AIEgens in nanoparticles, resulting in AIENPs with a highly restricted rotational environment. These NPs provide enhanced photostability and greater resistance to photobleaching compared to traditional organic fluorophores, high brightness, and reduced background interference compared to QDs and EuNPs due to their large Stokes shift. By tuning the emission properties of different AIEgens, Zhan et al. [28] developed a multiplex LFIA for mycotoxin aflatoxin B1 (AFB1) and zearalenone (ZEN), quantification in cereals with LODs of 0.006 and 0.026 ng/mL, respectively. The incorporation of a third AIEgen in the cited work allowed for strip validation in the control line. For bioconjugation, they opted for boronate affinity to sugars. Boronic acids can form reversible covalent bonds with cis-diols present on sugars such as mannose, galactose, and sialic acid, which are commonly found on the glycosylated Fc region of mAbs achieving a stable NP-mAb conjugate (see section Carbohydrate directed immobilization). Another notable characteristic of AIEgens is their ability to modify their structure to tune their excitation and emission, allowing their use to be adapted to available light sources, as Bian et al. did with AIE490 [3]. Additionally, the encapsulation of this AIEgen in polystyrene particles increased its fluorescence tenfold compared to the AIEgen in the form of free nanoaggregates, due to the hydrophobicity of the matrix shielding the dye from water-induced quenching. The EDC/NHS method was used for NP-mAb conjugation. Dendritic mesoporous silica nanoparticles (DMSNs) have also emerged as a promising platform alternative for AIEgen loading as presented by Leng et al. [41]. The large surface due to the porous architecture of this material was exploited to enhance the adsorption of the nanoprobe. A superficial coating layer of $FeCl_3$ with tannic acid made the system hydrophilic and allowed for visual detection due to the iron cation conferring a brownish color to the particles. The mAb used in the cited work were conjugated through noncovalent bonds such as electrostatic interactions and metal-ligand coordination.

Latex NPs can also serve as a support for anchoring fluorophores, converting them into fluorescent nanoprobes. For instance, Girmatsion et al. [67] used the blue protein phycocyanin, which emits red fluorescence under UV excitation for this purpose. In a single step and through an EDC activation process, these latex nanospheres were functionalized with the mentioned fluorescent protein and different mAbs allowing for multiplex mycotoxin determination. In a more recent study, Hang et al. [19] developed a multilayered nanostructure featuring AgNPs core coated with a silica shell, followed by a fluorophore layer and a final protective silica coating. This sandwich-like nanostructure not only safeguards the dye but also permits antibody bioconjugation by activating carboxyl groups with EDC/NHS. The metallic core enhances the fluorescent signal through the LSPR effect of silver.

Magnetic nanoparticles

Magnetic nanoparticles represent a distinct detection strategy. Traditionally they have been used for sample matrix cleaning and preconcentration, whereby antibody-conjugated nanoparticles capture the target analyte and are subsequently separated magnetically to

remove the sample matrix. The complexes are then resuspended in a cleaner or smaller volume medium, effectively increasing analyte concentration and enhancing assay sensitivity by reducing interference [9].

Recent advances have focused on integrating magnetic cores with optical amplification strategies. For example, Fe_3O_4@Au/PDA magnetic-plasmonic blackbody particles combine magnetic enrichment with enhanced colorimetric signal output, achieving LODs 41 times lower than those of traditional AuNP-LFIA for staphylococcal enterotoxin B detection [47]. Similarly, multilayered magnetic core dual-shell SERS tags (MDAu@Ag) integrate Fe_3O_4 cores with Au@Ag shells to provide both magnetic enrichment and strong SERS hotspots for multiplex veterinary drug detection at pg/mL levels [27]. Beyond colorimetric and SERS approaches (discussed in the next section), three-in-one multifunctional probes combining Fe_3O_4 cores with AuNP and QD layers enabled dual-mode LFIA combining colorimetric and fluorescent detection. Such probes demonstrate broad-spectrum viral detection capability, as shown in recent detection of SARS-CoV-2 and monkeypox virus using wheat germ agglutinin for universal glycoprotein recognition [48]. Additionally, Fe_3O_4@PEI/AuMBA@AgMBA nanocomposites allowed simultaneous magnetic enrichment and SERS detection of mycotoxins AFB1 and ZEN, achieving rapid analysis within 20 min [49]. These examples illustrate a clear trend toward multifunctional magnetic nanoprobes in LFIA, where magnetic cores facilitate rapid target enrichment and matrix cleanup, while attached plasmonic or fluorescent layers amplify detection signals. This synergistic integration enables high sensitivity, multiplexing capability, and robustness in complex matrices. Thus, while magnetism remains less frequently used as a standalone detection mode, its integration into hybrid nanoparticle systems is emerging as a promising strategy for next-generation LFIA development.

Other detection strategies

Recent advances demonstrate the successful integration of SERS and photothermal functionalities into LFIA through innovative nanoparticle designs, significantly enhancing assay sensitivity. In SERS-based LFIA, AuNPs or AgNPs are functionalized with Raman-active molecules such as rhodamine 6G, crystal violet, or 4-mercaptobenzoic acid (MBA), which provide unique spectral signatures for analyte identification [25,27,49,52]. Under laser excitation, these nanoparticles generate intense electromagnetic fields, amplifying Raman signals by several orders of magnitude and achieving detection limits far lower than those of traditional colorimetric assays. Recent studies have increasingly focused on metallic hybrid nanoparticles, leveraging synergistic enhancements in signal intensity, stability, and anti-interference performance. For example, gold–silver alloy hollow nanoshells (Au–Ag HNSs) functionalized with MBA as a Raman reporter were used in a tri-mode LFIA for detecting SARS-CoV-2 neutralizing antibodies, achieving an LOD of 20 ng/mL via SERS, 10 times more sensitive than visual detection [25]. Other examples include Au@Ag core–shell nanoparticles functionalized with rhodamine B and malachite green for multiplex detection of histamine and parvalbumin allergens in canned fish [50]. Similarly, gold nanostars coated with silver shells and MBA, enabled high-sensitivity SERS detection of influenza A virus antibodies by combining multi-branched Au cores (providing abundant hotspots) with Ag shells (enhancing electromagnetic fields) [51]. Likewise, bimetallic Au@Ag@Ag nanorods functionalized with 5,5′-dithio-bis-(2-nitrobenzoic acid) achieved an LOD of 0.0046 ng/mL for fipronil, outperforming similar immunoassays while minimizing ambient light interference [52].

Beyond SERS, photothermal detection in LFIA has been enhanced through both bimetallic combinations and morphological engineering. For instance, flower-like CuO@Ag bimetallic nanoparticles synthesized via a green metal self-reducing strategy (Cu_2O as both precursor and reductant) showed high photothermal efficiency (35.6 %) and excellent antibody coupling (∼99 %). When applied to clenbuterol detection, these nanostructures enabled a dual-readout system: traditional colorimetric visualization and photothermal mode based on near-infrared (808 nm) irradiation (Figure 3). The photothermal detection mode achieved a LOD of 0.131 ng/mL, approximately 20 times more sensitive than conventional AuNP-based LFIA [22].

In contrast to bimetallic designs, structural engineering of single-metal nanoparticles can also enhance photothermal performance. For example, coral-like hollow AuNPs templated by liposomes formed highly branched architectures that generated abundant plasmonic hotspots. This structural enhancement led to a sixfold improvement in the LOD over conventional spherical AuNPs [29].

Test lines may remain invisible at low analyte concentrations, complicating laser alignment for signal acquisition. This can be addressed by co-conjugating capture and control antibodies with AuNPs to render lines visible and facilitate accurate signal collection [25,50–52]. Overall, these studies highlight emerging trends toward metallic hybrid NPs for SERS enhancement, the application of bimetallic and morphological designs for photothermal amplification, and integration of multimodal detection within single nanoparticle systems.

Figure 3

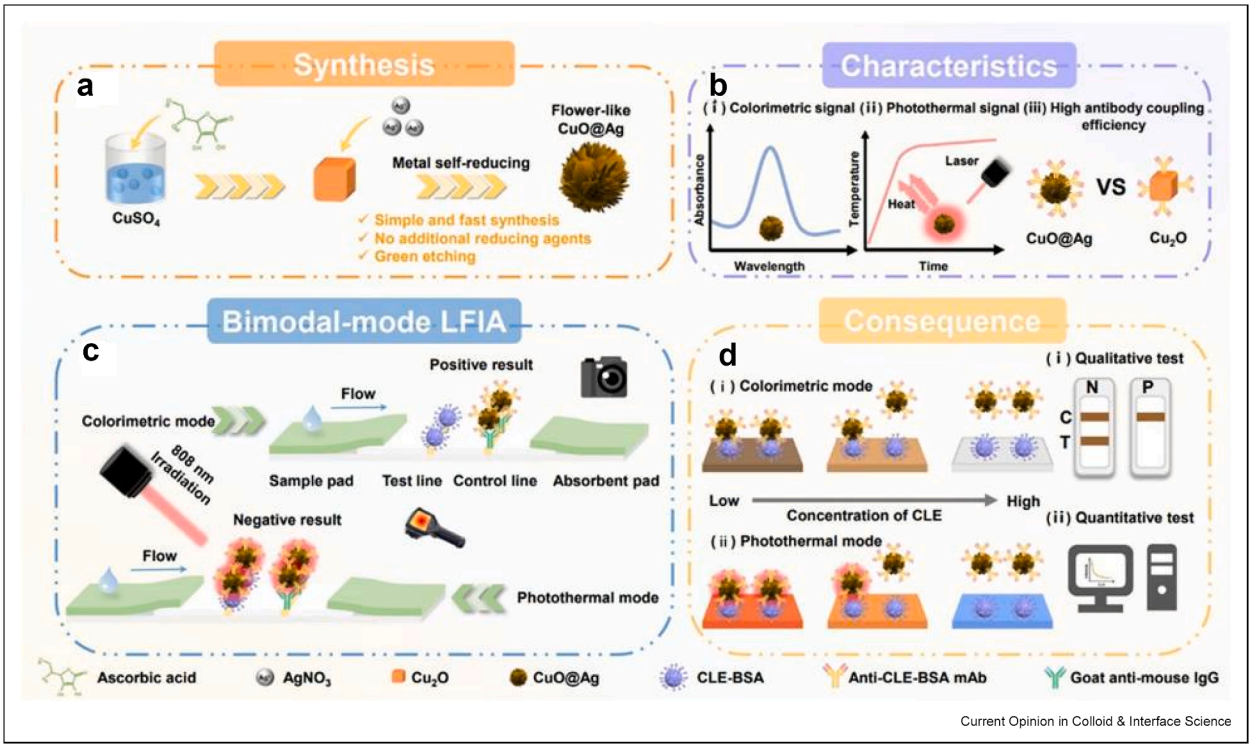

Schematic overview of a dual-mode LFIA using CuO@Ag flower-like nanoparticles for the detection of clenbuterol (CLE). **(a)** CuO@Ag nanoparticles are synthesized via a metal self-reduction process using ascorbic acid and $CuSO_4$, yielding bimetallic nanostructures with no additional reducing agents. **(b)** The resulting CuO@Ag exhibits strong colorimetric and photothermal responses as well as enhanced antibody coupling efficiency compared to Cu_2O alone. **(c)** The bimodal LFIA operates in colorimetric mode (visual detection) and photothermal mode (808 nm laser-based thermal signal), enabling improved signal readout. **(d)** This dual-mode approach allows both qualitative (i) and quantitative (ii) detection of CLE through changes in line intensity and temperature profiles at the test line. N: negative; P: positive; C: control line; T: test line. Ref. [22]. LFIA, lateral flow immunoassay.

Although not very common, electrochemical detection is another valid alternative for LFIA. Shi et al. developed a system for detecting α-fetoprotein (AFP), a diagnostic marker for liver cancer, using dendritic mesoporous silica nanospheres (DMSN) as a support matrix, where AuNPs were loaded into the pores [68]. The system was then coated with a silver shell, which acts as an electroactive redox reporter. The nanostructures were conjugated to antibodies via electrostatic interactions. In this electrochemical LFIA [20], Preechakasedkit et al. developed a laser-induced graphene-integrated electrode strip for the rapid detection of the foodborne pathogen *Salmonella typhimurium* This platform achieved exceptional sensitivity detecting as few as 1 CFU/10 mL, using AuNPs and Au^0 electrodeposition.

MXenes, a class of 2D nanosheets composed of transition metal carbides, nitrides, or carbonitrides, have also begun to attract attention in LFIA applications. Particularly, $Ti_3C_2T_x$ MXene exhibits high conductivity, biocompatibility, and versatile surface chemistry, making it ideal for signal amplification, target capture, and enhanced detection sensitivity in biosensors. While their use in electrochemistry has grown exponentially, their integration into LFIA platforms remains limited. A recent study [21] demonstrated how MXene's strong fluorescence quenching ability and reducing properties can be utilized as support for *in situ* formation and anchoring of AuNPs, creating a multifunctional nanomaterial exhibiting synergistic properties for both visual and fluorescence detection.

Overall, recent advances demonstrate that LFIA nanoprobes are evolving from simple optical labels into multifunctional hybrid systems capable of simultaneous target enrichment, capture, and multimodal detection. This shift is driven by the integration of bimetallic and metallic hybrid designs that provide synergistic SERS and photothermal enhancements, strategic morphological engineering to maximize plasmonic hotspots, and the coupling of magnetic enrichment with plasmonic or fluorescent readouts to improve sensitivity and robustness in complex matrices. Additionally, the emergence of eco-friendly synthesis approaches further reflects a

growing emphasis on sustainability nanoprobe development.

Immobilization strategies

The performance of LFIAs strongly depends on how recognition elements (generally antibodies) are immobilized onto the surface of nanoparticles. The choice of immobilization strategy affects not only the stability of the conjugate but also the orientation and availability of the antigen-binding sites, thereby influencing assay sensitivity and reproducibility. Broadly, immobilization can occur through noncovalent adsorption (physisorption) or via chemical or bioaffinity-driven bonding (chemisorption). Each approach presents distinct advantages and limitations, which are critical to consider in the context of specific assay formats and target analytes.

Physisorption

Physisorption remains one of the most commonly used method to immobilize recognition agents, such as antibodies, onto nanoparticles. Its simplicity avoids harsh chemical modifications, preserving antibody functionality, but lacks control over orientation and stability, which can reduce antigen-binding efficiency and assay reproducibility. Compared to covalent strategies, physisorption yields milder attachments without altering NP surfaces, though the resulting weaker binding can increase assay variability and reduce long-term stability.

Protein–NP interactions in physisorption are dynamic and initially driven by nonspecific forces, including electrostatic, hydrophobic, and van der Waals, and, over time, metal–sulfur interactions. Electrostatic interactions occur when charged NPs interact with oppositely charged regions on the protein. For instance, negatively charged citrate-stabilized AuNPs preferentially adsorb proteins with positively charged surface residues, especially at pH values below the protein's isoelectric point [13,38]. Hydrophobic interactions are significant with nonpolar surfaces or polymer-coated NPs, while hydrogen bonding becomes relevant for hydroxyl-rich surfaces such as silica [39]. Van der Waals forces are always present in protein–nanoparticle interactions, but their effect is enhanced when the protein surface conforms to the nanoparticle's surface, maximizing the contact area. In some cases, this surface-induced conformational change can even lead to partial or complete denaturation, altering the protein's biological function [39,40].

However, the outcome of physisorption is not always predictable and may vary significantly depending on the antibody's structure, origin, and solution conditions. For example, Mateos et al. [69] showed that a rabbit-derived anti-L1 cell adhesion molecule (L1CAM) antibody triggered immediate aggregation of citrate-capped AuNPs at low ionic strength, due to attractive Ab–Ab interactions amplified by nanoparticle binding. These interactions led to micron-sized protein aggregates and AuNP clusters. Increasing the ionic strength reversed the effect: Ab–Ab interactions became repulsive, aggregates dissolved, and stable Ab coronas formed. This case illustrates that physisorption can inadvertently promote antibody self-association and that colloidal behavior must be evaluated case-by-case as different antibody–NP combinations may behave unpredictably.

Metal–sulfur bonds typically form after initial physisorption as proteins undergo conformational changes exposing buried cysteine residues, which constitute only ~2 % of mammalian amino acids. Moreover, the extent of S–Au bond formation increases with cysteine content, reinforcing that covalent bonding plays a stabilizing rather than primary role in protein adsorption. Initially, thiol-containing proteins interact weakly with the NP surface [70], but over time, especially under alkaline conditions that promote thiol deprotonation, the S–H bond can break allowing the formation of stronger covalent metal–sulfur bonds [71]. Similar metal–sulfur interactions have been reported for silver, Pt, and palladium nanoparticles reflecting the broader relevance of metal–thiol chemistry in nanoparticle biointerfaces.

Au–S bond is usually described as covalent; however, its formation involves a complex interplay of covalent, ionic, and van der Waals interactions. A more accurate description is that of a resonance hybrid, exhibiting both dispersive force-dominating Au(0)-thiyl and covalent/ionic force-dominating Au(I)–thiolate character [71]. This nuanced nature contributes to its dynamic behavior under varying environmental conditions. While the Au–S bond is generally stable under ambient conditions, it is not irreversible. High temperatures can increase molecular motion, potentially breaking weaker dative bonds before covalent bonding is fully established. Additionally, ligand exchange can occur if competing thiol-containing molecules are present, leading to displacement of the initially adsorbed protein.

Recent studies continue to demonstrate the practical relevance of physisorption for diagnostic development. For instance, in food safety applications, dichlorvos pesticide was detected via AuNP physisorption at 16–108 μg/kg [14] and tetrodotoxin at 0.3 ng/mL [55]. In clinical diagnostics, a SARS-CoV-2 LFIA achieved 1 ng/mL detection using physisorbed antibodies [1]. Bisacodyl and related laxatives were detected at 1.4–10 ng/mL by leveraging concentrated AuNPs for enhanced physisorption efficiency [72]. Similarly, gold nanostars with physisorbed antibodies enabled ultrasensitive carbendazim detection down to 0.48 ng/mL [56]. These examples illustrate that despite its inherent limitations, physisorption remains a robust and scalable

immobilization strategy particularly when combined with optimized assay design and nanoparticle engineering.

Chemisorption

While physisorption strategies rely on noncovalent forces such as electrostatic, hydrophobic, and van der Waals interactions to anchor antibodies onto nanoparticle surfaces, chemisorption approaches involve the formation of deliberate chemical bonds in an effort to achieve stronger, more durable conjugation. Chemisorption typically requires chemical modification of the antibody, the nanoparticle surface, or both, to introduce reactive functional groups that enable covalent or bioaffinity-based attachment. These strategies are designed to maximize antigen-binding efficiency while minimizing nonspecific adsorption and antibody denaturation, often resulting in improved assay sensitivity and reproducibility. However, chemisorption methods tend to be more time-consuming and costly compared to physisorption, despite their advantage of allowing lower antibody consumption due to improved orientation [73]. In LFIAs, where robustness and minimal desorption are increasingly critical, chemisorption offers a route toward enhanced performance under challenging sample or storage conditions. This section examines the main chemisorption strategies currently employed or emerging in LFIA development, spanning amine-based covalent coupling, sulfhydryl-directed immobilization, carbohydrate-specific attachment, and bioaffinity-driven methods such as biotin–streptavidin interactions. Each strategy presents distinct implications for practical implementation in nanoparticle-based diagnostics.

Amine-based conjugations

This is one of the most widely used antibody–NP conjugation methods. It takes advantage of the abundance of primary amine groups, particularly lysine residue, on antibody surfaces. Carboxylated NPs are activated using EDC, often in combination with NHS or sulfo-NHS, to generate reactive NHS esters that covalently bond with antibody amines, creating stable amide linkages. The reaction proceeds optimally at around pH 7.4, where amine groups are sufficiently nucleophilic, and carboxyl groups remain deprotonated and reactive. Despite the enhanced efficiency, NHS esters are prone to hydrolysis in aqueous environments, requiring their prompt use after activation. Although chemically robust, EDC/NHS conjugation typically leads to random antibody orientation, since lysine residues are distributed throughout both the Fc and Fab regions. This randomness can impair antigen-binding efficiency by sterically hindering or misorienting the antigen recognition sites.

In current LFIA research, EDC/NHS chemistry remains a cornerstone, employed either to directly conjugate antibodies or as a preparatory step for ligand-based conjugation strategies. For instance, Ekman et al. used EDC/sulfo-NHS to conjugate anti-CA125 and anti-CA15-3 antibodies to $NaYF_4$-based UCNPs for dual-analyte detection [16]. Similarly, Chen et al. applied this chemistry to lanthanide-doped UCNPs targeting ZEN in cereals [74]. Wu et al. used EDC/NHS to conjugate anti-ciliary neurotrophic factor antibodies to carboxylated quantum dots [26], while Bian et al. reported its use in multicolor LFIA targeting SARS-CoV-2 using AIE-based polystyrene particles [3].

Despite its advantages, the limitations of random orientation and possible Fab inactivation have prompted more sophisticated uses of EDC/NHS as part of hybrid strategies. For example, instead of conjugating antibodies directly, EDC/NHS chemistry has been used to first attach protein G onto quantum dots, which then oriented the antibody through Fc binding, improving detection performance in neonatal respiratory distress diagnosis [75]. In other studies, such as those reported by Zhang et al. [28] and Xiong et al. [42], EDC/NHS served to anchor boronic acid ligands to the nanoparticle surface (e.g., 3-aminophenylboronic acid), enabling reversible and site-directed antibody attachment via boronate–diol interactions at the Fc glycan moieties. These indirect methods preserve antibody functionality and allow more predictable orientation.

Amine-based conjugation ensures durable, covalent attachment, making it valuable in complex environments. However, in LFIA, which operate under relatively mild conditions, such stability may not be critical. In many cases, physisorption (especially involving Au–S interactions) can be sufficient as long as antibody orientation and long-term stability are adequately controlled. A key advantage of EDC/NHS coupling in LFIA is its resistance to antibody displacement by proteins on the test line, such as cysteine-rich capture antibodies. Covalent amide bonds offer greater retention than dynamic physisorbed systems, which can suffer from competitive exchange and may lead to increased background or false positives. This is particularly relevant when test line antibodies have a higher cysteine content potentially allowing them to outcompete detection antibodies for binding the nanoparticle surface.

Sulfhydryl-based strategies

Sulfhydryl-based conjugation exploits the high affinity of thiol groups (–SH) for gold surfaces, forming stable Au–S bonds. Unlike physisorption, which involves noncovalent interactions such as electrostatic forces, van der Waals forces, and hydrogen bonding, sulfhydryl-based approaches aim for more stable and oriented immobilization through covalent linkage. However, since native antibodies lack free thiols due to stabilizing disulfide bridges, this strategy focuses on thiol generation. Two main approaches remain prevalent: (i) lysine

modification using reagents like 2-iminothiolane (Traut's reagent) or N-succinimidyl S-acetylthioacetate, and (ii) selective reduction of hinge region disulfides using reducing agents such as tris(2-carboxyethyl)phosphine (TCEP), dithiothreitol, or 2-mercaptoethylamine (2-MEA). Among these, TCEP has become the reducing agent of choice due to its non-thiol nature, avoiding competition with antibody thiols for gold binding and eliminating the need for post-reduction purification steps [43,54].

A notable innovation is the photochemical immobilization technique (PIT), which employs UV irradiation (254–280 nm) to cleave disulfide bonds selectively, generating free thiols without chemical reagents [36,76,77]. PIT has been applied for oriented antibody immobilization on planar gold surfaces in quartz crystal microbalance and fluorescence assays [78,79]. However, its direct application to LFIA has not yet been demonstrated, likely due to UV compatibility constraints with nitrocellulose membranes, presenting a promising area for future research particularly in developing UV-tolerant substrates or localized irradiation approaches.

Although both sulfhydryl-based strategies and physisorption may ultimately result in the formation of Au–S bonds, they differ fundamentally in how and when these bonds are established. In conventional physisorption, antibodies adsorb onto citrate-stabilized AuNPs through nonspecific electrostatic and hydrophobic interactions. Any subsequent covalent Au–S bond formation relies on slow and often incomplete conformational changes that expose buried cysteine residues, a process that is slow, heterogeneous, and poorly controlled. Moreover, the natural distribution and reactivity of cysteines in antibodies are variable and not inherently optimized for nanoparticle binding, resulting in conjugates with inconsistent orientation and limited stability. In contrast, sulfhydryl-based strategies involve the intentional generation or placement of reactive thiol groups, either by chemically reducing disulfide bonds (e.g., with TCEP to generate half-antibodies) or through site-specific cysteines engineering. These accessible thiols enable the direct, efficient, and robust Au–S bonds under controlled conditions. The resulting conjugates exhibit greater reproducibility, improved resistance to desorption, and more predictable antibody orientation. Importantly, the growing interest in non-antibody recognition agents such as aptamers or nanobodies in LFIAs has contributed to a renewed focus on sulfhydryl-based conjugation [54,80–82]. Thiol-modified aptamers are increasingly used in LFIA formats but require reduction of disulfide-linked dimers to expose active thiol groups for stable Au–S attachment. For instance, Tang et al. used TCEP to reduce oxidized thiol-modified DNA aptamers targeting tetrodotoxin, enabling efficient conjugation to AuNPs [82]. Similarly, Justo et al. designed a fully biotin-free LFIA for neutrophil gelatinase-associated lipocalin, where detection aptamers were functionalized with thioctic acid and conjugated directly to citrate-stabilized AuNPs via robust Au–S bonding [45].

An analogous strategy has been applied to nanobodies engineered with terminal cysteines, providing an ideal site for site-specific conjugation (Figure 4). However, expression in oxidative bacterial compartments often results in disulfide-linked dimers. Ayrton et al. addressed this by using TCEP to reduce dimeric nanobodies into monomeric forms bearing a single, free thiol, facilitating efficient and oriented AuNP attachment [54].

Carbohydrate directed immobilization

Carbohydrate-directed immobilization strategies exploit the presence of conserved N-linked glycans located in the Fc region of IgG antibodies to achieve site-selective conjugation onto nanoparticle surfaces. This spatially controlled approach is used to improve antibody orientation and functional display in biosensing platforms, including LFIA. By targeting glycan structures that are distal from the antigen-binding Fab domains, these strategies are designed to preserve antigen accessibility and enhance conjugate performance compared to random lysine- or cysteine-based methods.

Two principal approaches are commonly used for carbohydrate-directed immobilization; (1) oxidation of glycan residues in the Fc region to generate reactive aldehydes, and (2) boronate affinity interactions that bind native cis-diols. In the oxidation-based method, mild oxidizing agents such as sodium periodate ($NaIO_4$) are used to selectively oxidize the cis-diol groups of the glycan chains, generating aldehyde groups that can then react with nucleophilic moieties on the NP's surface such as primary amines or hydrazide groups. This reaction forms Schiff bases, which are then stabilized by reductive amination using sodium cyanoborohydride or borohydride, resulting in stable secondary amine linkages. For example, Yu et al. [33] oxidized antibodies against C-peptide using $NaIO_4$ and conjugated them to aminated polystyrene time-resolved microspheres through Schiff base formation. The resulting imine bonds were subsequently stabilized through reductive amination using sodium borohydride. The oriented conjugates enabled high sensitivity of C-peptide detection with a LOD of 0.005 ng/mL. Jiang et al. [83] applied a similar conjugation strategy to anti-Fc antibodies, which were covalently coupled to aminated polystyrene nanoparticles via reductive amination.

Figure 4

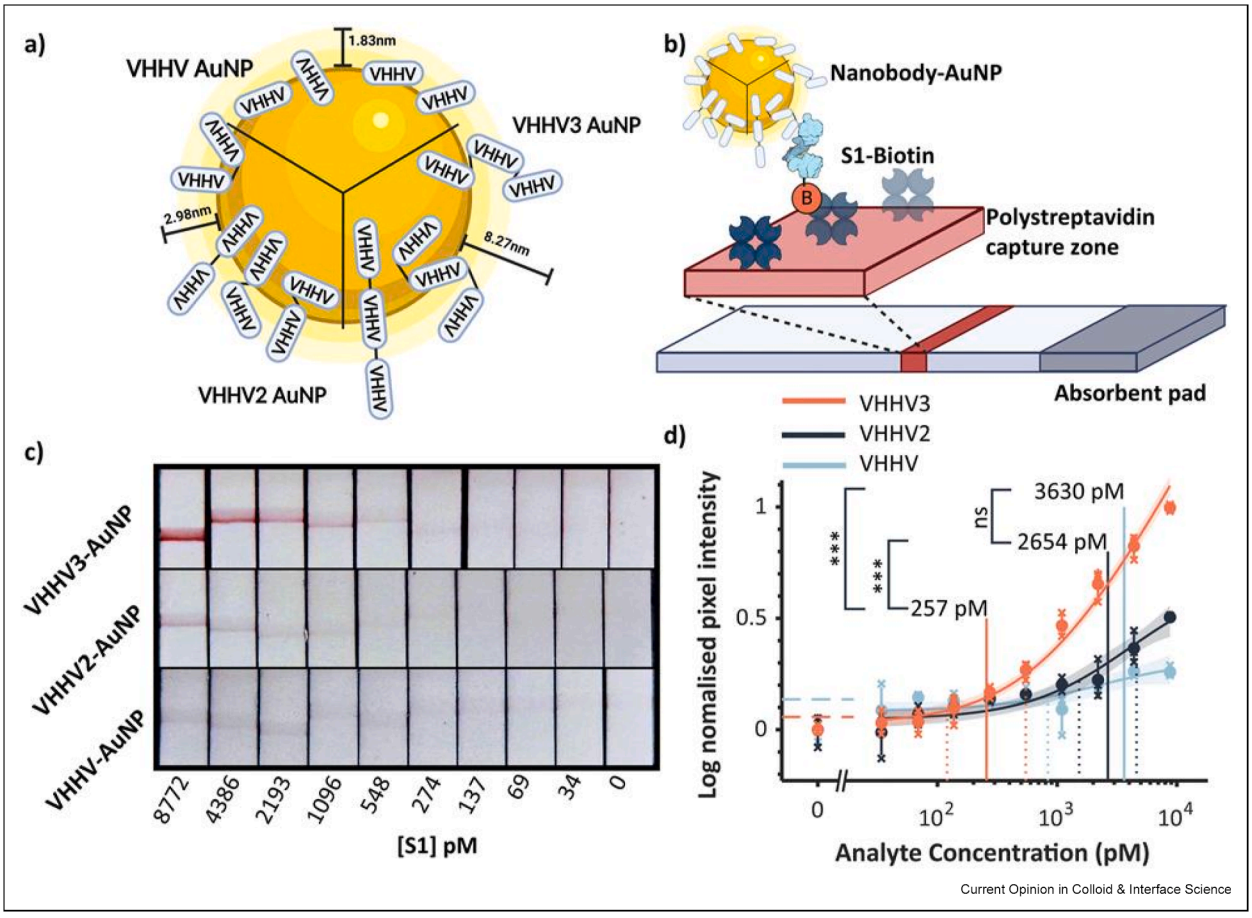

Evaluation of nanobody–AuNP conjugates for LFIA detection of SARS-CoV-2 S1 protein. **(a)** Scheme showing three distinct nanobody–AuNP conjugates with different nanobody orientations and surface densities. **(b)** Illustration of a direct LFA setup, where biotinylated S1 antigen is captured at the test line via polystreptavidin binding. **(c)** Representative test strips for each bioconjugate across a range of S1 concentrations. **(d)** Signal intensities plotted as a function of analyte concentration demonstrate varying detection sensitivities, with LODs determined by Langmuir fitting (solid lines) and 95 % confidence intervals (dashed lines). VHHV is the name of the nanobody used and the number refers to the quantity of nanobodies forming the chain, mono, bi, or trivalent, respectively. Reproduced from Ref. [54]. AuNPs, gold nanoparticles; LOD, limit of detection.

These particles then served as a modular platform for noncovalent capture of multiple Fc-containing antibodies, facilitating multiplexed detection.

On the other hand, boronate affinity-based immobilization avoids oxidation altogether by exploiting the reversible formation of boronate esters between PBA ligands and the native cis-diols present in the Fc-region glycans of antibodies [84]. This chemo-selective, dynamic covalent approach allows antibodies attachment to nanoparticle surfaces without chemical modification of the antibody itself, reducing complexity and minimizing the risk of functional impairment. Boronic acid ligands such as 3-aminophenylboronic acid or phenylboronic acid (PBA) are first covalently grafted onto carboxylated nanoparticles using EDC/NHS chemistry. The resulting boronate-functionalized nanoparticles then bind glycosylated antibodies through reversible boronate ester formation.

Lin et al. [34] demonstrated the use of boronic acid-functionalized quantum dot nanobeads (PBA-QBs) to achieve efficient antibody conjugation via Fc glycans. This approach yielded improved antibody orientation and significantly enhanced sensitivity in LFIA for hepatitis B surface antigen, with an LOD of 0.062 ng/mL while reducing antibody consumption compared to traditional EDC/NHS coupling. Xiong et al. [42] employed red-emitting AIENPs functionalized with PBA to conjugate antibodies for staphylococcal enterotoxin A detection, achieving an LOD of 0.04 ng/mL. Similarly, Zhang et al. [28] used differently colored PBA-AIENPs for multiplex detection of AFB1 (LOD: 0.006 ng/mL) and ZEN (LOD: 0.026 ng/mL),

demonstrating excellent selectivity and strong signal brightness.

Despite their benefits, carbohydrate-based conjugation strategies also have limitations. Oxidation protocols must be carefully optimized to avoid compromising antibody structure or antigen-binding function. The heterogeneity of glycosylation patterns among different antibody sources can also affect conjugation reproducibility. Furthermore, boronate affinity interactions are pH-dependent and reversible, which may limit their long-term stability without further stabilization such as crosslinking or optimization for use in buffered LFIA conditions [37].

Biotin–streptavidin coupling

The biotin—streptavidin coupling strategy is one of the most widely employed bioaffinity-based immobilization techniques in nanobiotechnology, owing to the exceptional strength and specificity of the fast interaction between biotin and streptavidin. This noncovalent interaction is among the strongest known in nature, with a dissociation constant in the femtomolar range (10^{-14} M) [85] and is highly stable under a wide range of experimental conditions. In this strategy, antibodies are first functionalized with biotin, typically through covalent attachment to lysine residues via NHS ester derivatives of biotin. The biotinylated antibodies are then immobilized onto streptavidin-coated nanoparticles or sensor surfaces. Biotinylation reagents are easily available commercially, are well-characterized and compatible with mild aqueous conditions eliminating the need for harsh chemical treatments. Additionally, since streptavidin contains four binding sites, it enables the construction of multivalent, highly stable bioconjugates, which can enhance both assay sensitivity and robustness. One of the main advantages of this method is its modularity: biotinylation can be directed specifically to defined regions of the antibody, such as the Fc domain, either through glycan oxidation followed by hydrazide—biotin coupling, or through site-specific enzymatic biotinylation using biotin ligase recognition sequences.

In many modern LFIA systems, the biotin—streptavidin interaction is not used to directly conjugate detection antibodies to nanoparticles but rather serves auxiliary roles, such as signal amplification, test line anchoring, or modular assembly. For example, in peptide-based noncompetitive LFIA systems, biotinylated anti-immunocomplex peptides are immobilized onto streptavidin—AuNPs to detect small molecules like deltamethrin [86]. In nanobody-based assays, biotinylated nanobodies can be modularly coupled to streptavidin-coated AuNPs prior to application (Figure 5) [46], while in bacterial detection systems, surface biotinylation of cells allows for universal capture using streptavidin—AuNPs [87]. In each of these applications, biotin acts as a versatile linker, enabling rapid probe generation. Additionally, several studies now apply the biotin—streptavidin system in CRISPR-Cas-based assays, where CRISPR stands for clustered regularly interspaced short palindromic repeats and Cas denotes CRISPR-associated proteins, programmable RNA-guided nucleases that recognizeand cleave specific nucleic acid sequences. In these assays, biotinylated DNA reporters are digested by activated Cas12a (or Cas13) enzymes following recognition of the target sequence, typically after isothermal amplification such as recombinase-assisted amplification (RAA). Cleavage of the biotin-DNA probe prevents its hybridization to capture probes on the test line, resulting in loss of signal, either a diminished colorimetric band or reduced fluorescence from streptavidin-functionalized AuNPs or QDs. Hence, the presence or absence of the test line reflects CRISPR-Cas—mediated reporter cleavage, providing a simple, low-cost, and highly specific nucleic-acid detection mechanism suitable for point-of-care applications [35,88].

Techniques for protein corona verification

There are several methods available to confirm the formation of a protein corona around nanoparticles. One of the simplest and most widely used techniques is dynamic light scattering, where an increase in hydrodynamic diameter suggests successful antibody adsorption or binding onto the nanoparticle surface. This increase typically ranges from 5 to 15 nm, consistent with the approximate dimension of an antibody molecule.

UV—Vis absorbance spectroscopy is particularly useful for characterizing nanoparticles that exhibit LSPR, such as gold or silver NPs. Protein adsorption typically leads to a red shift in the LSPR peak along with a decrease in its intensity, both of which are indicative of surface modification and corona formation.

For nanoparticles with surface charges (e.g., carboxylated NPs), zeta potential measurements can also provide evidence of protein corona formation. Upon antibody conjugation, the zeta potential usually becomes less negative due to the masking of surface charges by the adsorbed protein layer [3,91].

While these mentioned techniques effectively analyze electrostatic and physisorbed interactions, confirming covalent bond formation requires alternative characterization approaches. Fourier transform infrared (FTIR) spectroscopy and X-ray photoelectron spectroscopy (XPS) are commonly employed for this purpose. For example, in one study [92], FTIR, XPS, and cyclic voltammetry were used to analyze the interaction between citrate-coated silver nanoparticles and polyclonal antibodies against Staphylococcal enterotoxin B. The

Figure 5

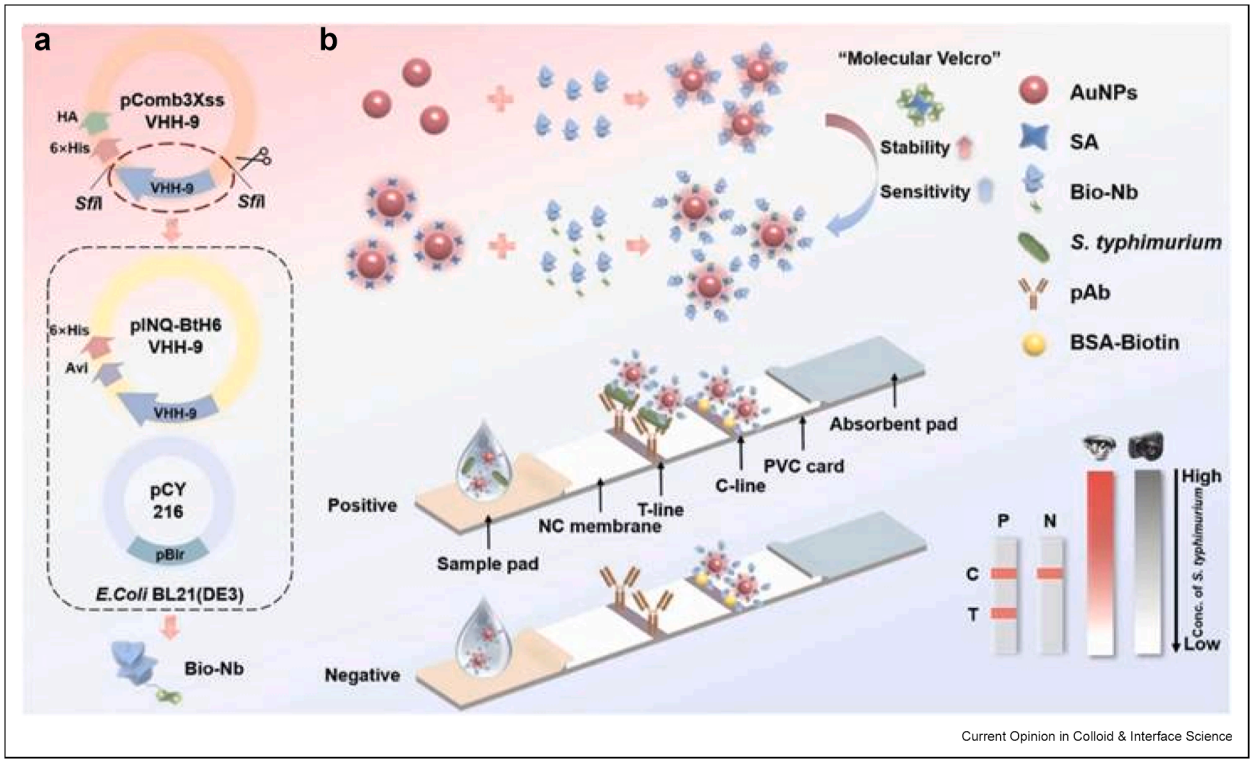

Design and application of a biotinylated nanobody-based LFIA for *Salmonella typhimurium* detection. **(a)** Schematic representation of the recombinant vector constructs used to express biotinylated nanobodies (Bio-Nb) in *E. coli*. **(b)** Overview of the LFIA platform employing AuNPs, streptavidin (SA) and biotinylated nanobodies, forming a "molecular Velcro" complex that enhances stability and sensitivity. Detection of *S. typhimurium* is achieved via formation of test (T) and control **(c)** lines on the nitrocellulose (NC) membrane. Reproduced from Ref. [46]. AuNPs, gold nanoparticles; *E. coli, Escherichia coli; LFIA, lateral flow immunoassay.*

voltammogram revealed the absence of Ag^{+} peaks upon antibody binding, suggesting complete surface coverage, while FTIR spectra revealed characteristic amide bands confirming peptide bond formation. XPS further validated the presence of these bonds, providing comprehensive evidence of successful covalent conjugation.

Although transmission electron microscopy (TEM) and scanning electron microscopy (SEM) are not typically used to directly visualize protein layers due to the low electron density or organic materials, they remain valuable tools for confirming nanoparticle morphology and size before and after surface functionalization. High-resolution TEM is particularly useful for visualizing interplanar spacings within metallic nanostructures, ensuring proper hybrid nanoparticle formation [90].

X-ray diffraction provides complementary information on the crystallographic structure and atomic arrangement of nanoparticles [90] Additionally, energy-dispersive X-ray spectroscopy (EDS) coupled with TEM or SEM allows elemental mapping, verifying the presence of different metals in hybrid nanoparticles [49] or confirming protein conjugation by detecting characteristic nitrogen peaks originating from the protein layer [60].

Conclusion

Central to LFIA performance is the formation of the protein corona, where immobilization strategies, ranging from physisorption to chemisorption via amine-, sulfhydryl-, or carbohydrate-directed coupling, as well as bioaffinity approaches, dictate antibody orientation, stability, and antigen-binding efficiency. Traditionally, chemisorption and bioaffinity-based methods have been considered superior due to their strong, covalent, and site-directed binding, which improves conjugate stability and theoretically enhances assay sensitivity. However, a critical examination of recent studies (Table 1) challenges the prevailing assumption that chemisorption invariably outperforms physisorption in practical LFIA applications. Emerging evidence indicates that physisorption, despite its simplicity and reliance on noncovalent interactions, often achieves comparable or

even superior detection limits. The examples discussed in this review highlight that, when assay conditions such as pH, ionic strength, and nanoparticle size are optimized physisorption can achieve extremely low detection limits. However, direct comparisons among conjugation methods are not straightforward as multiple parameters beyond the assay (including nanoparticle architecture, assay format, and detection modality) influence final performance and vary across studies.

Overall, the data suggest that physisorption and chemisorption should not be viewed as strictly hierarchical but rather as complementary strategies. Physisorption remains advantageous for its operational ease, low cost, and minimal chemical processing, making it particularly suitable for scalable, rapid LFIA production. Conversely, chemisorption and bioaffinity strategies, while more complex, become indispensable when stability, controlled antibody orientation, or multiplexing capabilities under challenging conditions are critical. These methods are especially valuable, in assays targeting small molecules, where antigen-binding sites accessibility is critical, or in complex biological matrices containing thiol-rich proteins that could displace weakly bound antibodies.

Beyond immobilization methods, emerging trends in LFIA point toward the design of multifunctional hybrid nanoparticles integrating magnetic cores for target preconcentration, plasmonic or fluorescent shells for signal enhancement, and catalytic or photothermal properties enabling alternative readouts such as SERS, photothermal, and electrochemical detection [6,17,20–22,31,76]. In parallel, morphological engineering (nanostars, coral-like hollow AuNPs, and flower-like bimetallics) concentrates plasmonic hotspots and increases probe loading, boosting sensitivity, and quantitative performance [23,29,51,56]. Notably, in SERS and plasmon-enhanced fluorescence, the aspect ratio of anisotropic labels (e.g., nanorods, nanostars, alloy nanoshells) tunes the localized surface plasmon resonance and near-field confinement, leading to pronounced changes in Raman enhancement and fluorescence amplification [52]. In routine practice, however, most LFIAs still employ spherical labels and tune size to balance transport and signal: within an optimal size window, AuNPs accumulate at the test line and, via strong LSPR, yield an intense red band suitable for naked-eye inspection and reader-based quantification; oversized AuNPs are prone to aggregation, whereas smaller AuNPs exhibit weaker LSPR and reduced sensitivity [10,93]. Very large labels can also slow capillary migration and increase steric crowding at the test region. However, detailed size–shape optimization has been extensively covered in the earlier literature and is beyond the scope of this opinion review.

A pragmatic shift worth mentioning is the broader use of recombinant/synthetic biorecognition elements in place of animal IgGs. Nanobodies and affibodies are microbially produced, compact (allowing higher surface densities), and support modular coupling (His/Avi/biotin; streptavidin systems) while maintaining assay sensitivity [35,46,53,54]. Aptamers and designed peptides likewise avoid animal immunization and are synthesized at scale [45,55,78,80,81,86], delivering robust LFIA performance across pathogens, toxins, and small molecules.

Looking ahead, the future of LFIA nanoprobes is probably less about inventing new labels and more about turning promising concepts into robust, manufacturable products. Priorities include scaling conjugation and strip fabrication to automated, in-line processes; engineering shelf-stable formulations that tolerate heat, humidity, and diverse matrices; and establishing standardized benchmarking to delineate when optimized physisorption is enough versus oriented chemisorption. Equally important is a portable reader apparatus (smartphone or handheld) supporting on-strip calibration with spectrally separated labels with validated deconvolution and cross-reactivity panels. Sustainable choices such as recombinant binders, lower precious metal loading, water-based syntheses, and end-of-life recovery should also go together with cost-down manufacturing to expand access.

Declaration of competing interest

The authors declare that they have no known competing financial interests or personal relationships that could have appeared to influence the work reported in this paper.

Acknowledgments

The work was indeed supported by the "Italian Ministry of University and Research (MUR) within the Next-Generation EU-MUR PNRR initiative: Extended Partnership on Emerging Infectious Diseases (Project no. PE00000007, INF-ACT.

Data availability

No data was used for the research described in the article.

References

Papers of particular interest, published within the period of review, have been highlighted as:

* of special interest
** of outstanding interest

1. Prakashan D, Shrikrishna NS, Byakodi M, Nagamani K, Gandhi S: **Gold nanoparticle conjugate-based lateral flow immunoassay (LFIA) for rapid detection of RBD antigen of SARS-CoV-2 in clinical samples using a smartphone-based application**. *J Med Virol* 2023, **95**, https://doi.org/10.1002/jmv.28416.

2. Chen J, Luo P, Liu Z, He Z, Pang Y, Lei H, *et al*.: **Rainbow latex microspheres lateral flow immunoassay with smartphone-based device for simultaneous detection of three mycotoxins in cereals**. *Anal Chim Acta* 2022, **1221**, 340138, https://doi.org/10.1016/J.ACA.2022.340138.

3. Bian L, Li Z, He A, Wu B, Yang H, Wu Y, *et al*.: **Ultrabright nanoparticle-labeled lateral flow immunoassay for detection of anti-SARS-CoV-2 neutralizing antibodies in human serum**. *Biomaterials* 2022, **288**, 121694, https://doi.org/10.1016/J.BIOMATERIALS.2022.121694.

4. Chen C, Duan S, Ji J, Wu M, Yang Z, Cai M, *et al*.: **Structured protein probes modified with selenium nanoparticle for 1-minute measurement of SARS-CoV-2 antigen**. *Biosens Bioelectron* 2025, **268**, https://doi.org/10.1016/j.bios.2024.116878.

5. Liang JF, Li X, Huang B, Pan Y, Zhuang Z, Ye Q, *et al*.: **Rapid, on-site quantitative determination of mycotoxins in grains using a multiple time-resolved fluorescent microsphere immunochromatographic test strip**. *Biosens Bioelectron* 2024, **258**, https://doi.org/10.1016/j.bios.2024.116357.

6. Jin B, Ma B, Mei Q, Xu S, Deng X, Hong Y, *et al*.: **Europium nanoparticle-based lateral flow strip biosensors combined with recombinase polymerase amplification for simultaneous detection of five zoonotic foodborne pathogens**. *Biosensors (Basel)* 2023, **13**:652, https://doi.org/10.3390/BIOS13060652/S1.

7. Mei Q, Ma B, Li J, Deng X, Shuai J, Zhou Y, *et al*.: **Simultaneous detection of three nitrofuran antibiotics by the lateral flow immunoassay based on europium nanoparticles in aquatic products**. *Food Chem* 2024, **439**, https://doi.org/10.1016/j.foodchem.2023.138171.

8. Fu Y, Song Y, Yang Z, Ruan X, Lin Y, Du D: **Rapid and sensitive detection of wood smoke exposure biomarkers using europium fluorescent nanoparticle label/lateral flow immunoassay**. *Talanta* 2025, **291**, https://doi.org/10.1016/j.talanta.2025.127760.

9. Hua Q, Liu Z, Wang J, Liang Z, Zhou Z, Shen X, *et al*.: **Magnetic immunochromatographic assay with smartphone-based readout device for the on-site detection of zearalenone in cereals**. *Food Control* 2022, **134**, 108760, https://doi.org/10.1016/J.FOODCONT.2021.108760.

10. Prakashan D, Kolhe P, Gandhi S: **Design and fabrication of a competitive lateral flow assay using gold nanoparticle as capture probe for the rapid and on-site detection of penicillin antibiotic in food samples**. *Food Chem* 2024, **439**, https://doi.org/10.1016/j.foodchem.2023.138120.

11. Oliveira BB, Ferreira D, Fernandes AR, Baptista PV: **Engineering gold nanoparticles for molecular diagnostics and biosensing**. *Wiley Interdiscip Rev Nanomed Nanobiotechnol* 2023, **15**, https://doi.org/10.1002/WNAN.1836.

12. Ielo I, Rando G, Giacobello F, Sfameni S, Castellano A, Galletta M, *et al*.: **Synthesis, chemical–physical characterization, and biomedical applications of functional gold nanoparticles: a review**. *Molecules* 2021, **26**:5823, https://doi.org/10.3390/MOLECULES26195823.

13. Zhang L, Mazouzi Y, Salmain M, Liedberg B, Boujday S: **Antibody-gold nanoparticle bioconjugates for biosensors: synthesis, characterization and selected applications**. *Biosens Bioelectron* 2020, **165**, https://doi.org/10.1016/j.bios.2020.112370.

14. * Jia BZ, Liu YY, Chen FY, Tongchai P, Yadoung S, Wongta A, *et al*.: **Lateral flow immunochromatographic assay for rapid detection of dichlorvos residue in fruits and vegetables**. *Food Chem X* 2025, **28**, https://doi.org/10.1016/j.fochx.2025.102613.
This publication presents a gold nanoparticle-based LFIA for detecting dichlorvos pesticide residues in food samples. The assay uses physisorption of monoclonal antibodies onto colloidal gold, optimized through pH adjustment and BSA blocking. The study validates the LFIA's performance across six produce matrices, achieving detection limits below regulatory thresholds, with excellent accuracy, precision, and strong agreement with GC–MS/MS results. It exemplifies the practical efficacy of physisorption-based conjugates for robust, cost-effective, real-world diagnostics.

15. Ding M, Dou L, Bu T, Li Z, Mao Y, Dang M, *et al*.: **Nanometal surface energy transfer-based lateral flow immunoassay for T2 toxin detection**. *Biosens Bioelectron* 2025, **267**, https://doi.org/10.1016/j.bios.2024.116779.

16. Ekman M, Salminen T, Raiko K, Soukka T, Gidwani K, Martiskainen I: **Spectrally separated dual-label upconversion luminescence lateral flow assay for cancer-specific STn-glycosylation in CA125 and CA15-3**. *Anal Bioanal Chem* 2024, **416**:3251–3260, https://doi.org/10.1007/s00216-024-05275-z.

17. Chen C, Cao J, Wang X, Chai Q, Zhang Y, Chen H, *et al*.: **A novel dual-flux immunochromatographic test strip based on luminescence resonance energy transfer for simultaneous detection of ochratoxin A and deoxynivalenol**. *Microchim Acta* 2022, **189**:1–12, https://doi.org/10.1007/s00604-022-05561-6.

18. Zhang G, Yu S, Peng J, Xiong Y, Hu L, Lai W: **Novel reporter based on Aggregation-induced emission Luminogens for lateral flow immunoassay: a mini review**. *TrAC, Trends Anal Chem* 2025, **183**, https://doi.org/10.1016/j.trac.2024.118098.

19. Hang Y, Wang A, Tan W, Bess K, Eaton A, Wu N: **Plasmon-enhanced fluorescence paper lateral flow strip for point-of-care testing of SARS-CoV-2 antigens**. *Anal Chem* 2025, **97**:1221–1228, https://doi.org/10.1021/ACS.ANALCHEM.4C04697.

20. Preechakasedkit P, Panphut W, Lomae A, Wonsawat W, Citterio D, Ruecha N: **Dual colorimetric/electrochemical detection of Salmonella typhimurium using a laser-induced graphene integrated lateral flow immunoassay strip**. *Anal Chem* 2023, **95**:13904–13912, https://doi.org/10.1021/ACS.ANALCHEM.3C02252.

21. Deng Y, Wang Y, Lin M, Chen Y, Qian ZJ, Liu J, *et al*.: **High-density Au anchored to Ti3C2-based colorimetric-fluorescence dual-mode lateral flow immunoassay for all-domain-enhanced performance and signal intercalibration**. *Anal Chem* 2024, **96**:5106–5114, https://doi.org/10.1021/acs.analchem.3c04550.

22. Ma J, Yin X, Cheng Y, Wang C, Wu Q, Zhang Q, *et al*.: **Metal self-reducing triggered green etching for the CuO@Ag composite synthesis and its application in high-sensitive lateral flow immunoassay**. *Chem Eng J* 2024, **498**, 155341, https://doi.org/10.1016/J.CEJ.2024.155341.

23. Yang H, He Q, Chen Y, Shen D, Xiao H, Eremin SA, *et al*.: **Platinum nanoflowers with peroxidase-like property in a dual immunoassay for dehydroepiandrosterone**. *Microchim Acta* 2020, **187**:1–12, https://doi.org/10.1007/S00604-020-04528-9.

24. Mussin J, Giusiano G, Porras JC, Corredor Sanguña LH, Pividori MI: **Carbon nanoparticle–based lateral flow assay for the detection of specific double-tagged DNA amplicons of Paracoccidioides spp**. *Microchim Acta* 2024, **191**:1–8, https://doi.org/10.1007/S00604-024-06367-4.

25. ** Zhao T, Liang P, Ren J, Zhu J, Yang X, Bian H, *et al*.: **Gold-silver alloy hollow nanoshells-based lateral flow immunoassay for colorimetric, photothermal, and SERS tri-mode detection of SARS-CoV-2 neutralizing antibody**. *Anal Chim Acta* 2023, **1255**, 341102, https://doi.org/10.1016/J.ACA.2023.341102.
This paper introduces a tri-mode lateral flow immunoassay using gold-silver alloy hollow nanoshells (Au–Ag HNSs) as multifunctional labels for simultaneous colorimetric, photothermal, and SERS detection of SARS-CoV-2 neutralizing antibodies in serum. Antibodies were covalently conjugated to the Au–Ag HNSs via carbodiimide (EDC/NHS) chemistry targeting carboxyl groups on the nanoparticle surface. The resulting probes showed superior optical properties, high photothermal conversion efficiency, and signal amplification. The assay achieved LODs down to 20 ng/mL and demonstrated excellent reproducibility and stability.

26. Wu Y, Zhang Y, Hu Y, Jiang N, Patel RP, Yetisen AK, *et al*.: **Fluorescent quantum dots based lateral flow assay for rapid quantitative detection of ciliary neurotrophic factor in glaucoma**. *Adv Mater Technol* 2024, **9**, 2400238, https://doi.org/10.1002/admt.202400238.

27. Tu J, Wu T, Yu Q, Li J, Zheng S, Qi K, *et al*.: **Introduction of multilayered magnetic core–dual shell SERS tags into lateral flow immunoassay: a highly stable and sensitive method for the simultaneous detection of multiple veterinary drugs in**

complex samples. *J Hazard Mater* 2023, **448**, 130912, https://doi.org/10.1016/J.JHAZMAT.2023.130912.

28. Zhang Y, Chen G, Chen X, Wei X, Shen X ang, Jiang H, *et al*.: **Aggregation-induced emission nanoparticles facilitating multicolor lateral flow immunoassay for rapid and simultaneous detection of aflatoxin B1 and zearalenone**. *Food Chem* 2024, **447**, https://doi.org/10.1016/j.foodchem.2024.138997.

29. * Xiao X, Yu S, Zhang G, Chen Z, Hu H, Lai X, *et al*.: **Efficient photothermal sensor based on coral-like hollow gold nanospheres for the sensitive detection of sulfonamides**. *Small* 2024, **20**, 2307764, https://doi.org/10.1002/SMLL.202307764.
This study presents a novel, green synthesis route for CuO@Ag composite nanoparticles via metal self-reduction and etching. The authors demonstrate their use as colorimetric LFIA labels for detecting clenbuterol and ractopamine in food. Antibody conjugation was achieved using EDC/NHS activation of carboxyl groups on the nanoparticle surface. The high optical contrast and uniformity of the composite probes, combined with effective covalent conjugation, enabled sub-ng/mL sensitivity and excellent performance in real matrices.

30. Li W, Yang X, Wang D, Xie J, Wang S, Rong Z: **A handheld fluorescent lateral flow immunoassay platform for highly sensitive point-of-care detection of methamphetamine and tramadol**. *Talanta* 2024, **277**, https://doi.org/10.1016/j.talanta.2024.126438.

31. Li D, Ao L, Hu R, Zhang X, Huang L, Jiang C, *et al*.: **Kiwi-inspired rational nanoarchitecture with intensified and discrete magneto-fluorescent functionalities for ultrasensitive point-of-care immunoassay**. *Small* 2024, **20**, 2402676, https://doi.org/10.1002/smll.202402676.

32. Wen Z, Hu X, Yan R, Wang W, Meng H, Song Y, *et al*.: **A reliable upconversion nanoparticle-based immunochromatographic assay for the highly sensitive determination of olaquindox in fish muscle and water samples**. *Food Chem* 2023, **406**, https://doi.org/10.1016/j.foodchem.2022.135081.

33. Yu B, Cui Y, Mao X, Li Z, Li Z, Shi G: **A time-resolved fluorescence lateral flow immunochromatographic assay based on oriented immobilized antibodies for the ultrasensitive detection of C-peptides in human serum**. *Anal Chim Acta* 2022, **1208**, https://doi.org/10.1016/j.aca.2022.339833.

34. Lin T, Huang X, Guo L, Zhou S, Li X, Liu Y, *et al*.: **Boronate affinity-assisted oriented antibody conjugation on quantum dot nanobeads for improved detection performance in lateral flow immunoassay**. *Microchem J* 2021, **171**, https://doi.org/10.1016/j.microc.2021.106822.

35. Wang X, Sun T, Shen W, Liu M, Liu W, Zuo H, *et al*.: **A lateral flow immunochromatographic assay based on nanobody-oriented coupling strategy for aflatoxin B1 detection**. *Sensor Actuator B Chem* 2023, **394**, https://doi.org/10.1016/j.snb.2023.134419.

36. Neves-Petersen MT, Snabe T, Klitgaard S, Duroux M, Petersen SB: **Photonic activation of disulfide bridges achieves oriented protein immobilization on biosensor surfaces**. *Protein Sci* 2006, **15**:343–351, https://doi.org/10.1110/ps.051885306.

37. * Li J, Li X, Wang Y, Zhou Q, Shi G: **Utilization of Fc-specific peptide to orientally immobilize antibodies markedly improves the analytical performance of lateral flow immunoassay strips for aflatoxin B1**. *Microchem J* 2025, **208**, https://doi.org/10.1016/j.microc.2024.112404.
This study presents a chemisorption-based strategy for oriented antibody immobilization in LFIA using a synthetic Fc-binding peptide. The peptide was covalently attached to europium nanoparticles via EDC/NHS chemistry, allowing site-selective capture of antibodies through their Fc domain. This approach preserved the antigen-binding (Fab) sites and enabled enhanced target accessibility. The resulting LFIA exhibited a 10-fold improvement in sensitivity for aflatoxin B1 detection and a 4-fold increase in signal-to-noise ratio compared to random immobilization. This work exemplifies how covalent and oriented conjugation can significantly enhance assay performance, particularly when antigen binding efficiency is critical.

38. Sotnikov DV, Berlina AN, Ivanov VS, Zherdev AV, Dzantiev BB: **Adsorption of proteins on gold nanoparticles: one or more layers?** *Colloids Surf B Biointerfaces* 2019, **173**:557–563, https://doi.org/10.1016/j.colsurfb.2018.10.025.

39. Lundqvist M, Sethson I, Jonsson BH: **Protein adsorption onto silica nanoparticles: conformational changes depend on the particles' curvature and the protein stability**. *Langmuir* 2004, **20**:10639–10647, https://doi.org/10.1021/la0484725.

40. Monopoli MP, Åberg C, Salvati A, Dawson KA: **Biomolecular coronas provide the biological identity of nanosized materials**. *Nat Nanotechnol* 2012, **7**:779–786, https://doi.org/10.1038/nnano.2012.207.

41. Leng Y, Wang X, Li W, Lin X, Li X, Huang X: **Enabling ultrahigh loading of AIEgens through alkyne-amine click reactions for highly sensitive colorimetric-fluorescent dual-readout lateral flow immunoassay**. *Sensor Actuator B Chem* 2025, **432**, 137473, https://doi.org/10.1016/J.SNB.2025.137473.

42. Xiong H, Chen P, Chen X, Shen X, Huang X, Xiong Y, *et al*.: **Aggregation-induced red emission nanoparticle-based lateral flow immunoassay for highly sensitive detection of staphylococcal enterotoxin A**. *Toxins (Basel)* 2023, **15**, https://doi.org/10.3390/toxins15020113.

43. Conrad M, Proll G, Builes-Münden E, Dietzel A, Wagner S, Gauglitz G: **Tools to compare antibody gold nanoparticle conjugates for a small molecule immunoassay**. *Microchim Acta* 2023, **190**, https://doi.org/10.1007/s00604-023-05637-x.

44. Wu P, Song J, Zuo W, Zhu J, Meng X, Yang J, *et al*.: **A universal boronate affinity capture-antibody-independent lateral flow immunoassay for point-of-care glycoprotein detection**. *Talanta* 2023, **265**, https://doi.org/10.1016/j.talanta.2023.124927.

45. Justo CAC, Skouridou V, Cools P, Mulinganya G, Ibáñez-Escribano A, O'Sullivan CK: **Biotin/avidin-free sandwich aptamer-based lateral flow assay (ALFA) for the diagnosis of Trichomonas vaginalis**. *Sens Diagn* 2025, **4**:216–228, https://doi.org/10.1039/d4sd00342j.

46. Wang J, Shi L, Jing Y, Wang X, Liu X, Li S, *et al*.: **"Molecular Velcro": design of coupled AuNPs with streptavidin-biotin immobilized nanobody in lateral flow immunoassay for sensitive Salmonella typhimurium detection**. *Sensor Actuator B Chem* 2025, **435**, https://doi.org/10.1016/j.snb.2025.137604.

47. Sun J, Wu Y, Fan X, Peng J, Wang X, Xiong Y, *et al*.: **Magnetic-plasmonic blackbody enhanced lateral flow immunoassay of staphylococcal enterotoxin B**. *Food Chem* 2025, **465**, 142130, https://doi.org/10.1016/J.FOODCHEM.2024.142130.

48. Wu T, Liu Y, Zhou S, Li J, Sun G, Gu B, *et al*.: **Wheat germ agglutinin-modified "three-in-one" multifunctional probe driven broad-spectrum and flexible immunochromatographic diagnosis of viruses with high sensitivity**. *Small* 2025, **21**, https://doi.org/10.1002/SMLL.202406053.

49. Yin L, Cai J, Ma L, You T, Arslan M, Jayan H, *et al*.: **Dual function of magnetic nanocomposites-based SERS lateral flow strip for simultaneous detection of aflatoxin B1 and zearalenone**. *Food Chem* 2024, **446**, 138817, https://doi.org/10.1016/J.FOODCHEM.2024.138817.

50. * Fernández-Lodeiro C, González-Cabaleiro L, Vázquez-Iglesias L, Serrano-Pertierra E, Bodelón G, Carrera M, *et al*.: **Au@Ag core-shell nanoparticles for colorimetric and surface-enhanced Raman-Scattering-Based multiplex competitive lateral flow immunoassay for the simultaneous detection of histamine and parvalbumin in fish**. *ACS Appl Nano Mater* 2024, **7**:498–508, https://doi.org/10.1021/ACSANM.3C04696.
This work reports a dual-mode LFIA using Au@Ag core–shell nanoparticles for simultaneous colorimetric and SERS detection of the SARS-CoV-2 spike protein. Antibodies were immobilized via passive adsorption onto the bimetallic surface, leveraging the high optical contrast and SERS activity of the nanostructures. The platform enables rapid, sensitive, and reproducible viral antigen detection, highlighting the potential of physisorption-based dual-mode nanoprobes in biosensing.

51. Li J, Liu M, Zhu J, Jiao Y, Zeng J: **Ag-Coated Au nanostar-based lateral flow immunoassay for highly sensitive influenza A virus antibody detection in colorimetric and surface-enhanced Raman scattering (SERS) modes**. *Talanta* 2025, **285**, 127351, https://doi.org/10.1016/j.talanta.2024.127351.

52. Serebrennikova KV, Komova NS, Barshevskaya LV, Zherdev AV, Dzantiev BB: **Highly sensitive SERS-based lateral flow**

immunoassay of fipronil using bimetallic Au@Ag@Ag nanorods. *Microchim Acta* 2024, **191**:1–13, https://doi.org/10.1007/s00604-024-06811-5.

53. Sadler CJ, Creamer A, Giang KA, Darmawan KK, Shamsabadi A, Richards DA, *et al*.: **Adding a twist to lateral flow immunoassays: a direct replacement of antibodies with helical affibodies, from selection to application**. *J Am Chem Soc* 2025, **147**, https://doi.org/10.1021/jacs.4c17452.

This work presents a complete workflow for replacing immunoglobulin antibodies with engineered helical affibodies in LFIAs. Affibody candidates targeting SARS-CoV-2 spike protein were selected via phage display, expressed with His-tags, and directly conjugated to gold nanoparticles. The resulting LFIA enabled sub-nanogram detection of spike protein in human saliva. Molecular dynamics simulations revealed that affibody dimerization promotes compact, stable conjugates on AuNPs, enhancing signal intensity. This study showcases affibodies as robust, modular biorecognition elements that enable non-covalent but oriented and high-performance conjugation strategies for LFIA applications.

54. Ayrton JP, Ho C, Zhang H, Chudasama V, Frank S, Thomas MR: **Multivalent nanobody engineering for enhanced physisorption and functional display on gold nanoparticles**. *Nanoscale* 2024, **16**:19881–19896, https://doi.org/10.1039/d4nr02762k.

This study demonstrates that protein engineering can substantially enhance the effectiveness of physisorption onto gold nanoparticles. The authors designed trivalent nanobodies with optimized surface charge and multivalent presentation, enabling stronger and more stable adsorption to citrate-capped AuNPs even under physiological ionic strength. Using cryo-TEM, SPR, and functional ELISA-LFIA formats, they show that these engineered nanobodies maintain binding activity and colloidal stability, outperforming monovalent forms. This work highlights how tailoring bioreceptor architecture can elevate simple physisorption-based conjugation to rival the performance of covalent strategies

55. Díaz-Avello UG, Skouridou V, Shkembi X, Reverté J, Mandalakis M, Peristeraki P, *et al*.: **Aptamer-antibody sandwich lateral flow test for rapid visual detection of tetrodotoxin in pufferfish**. *Sci Total Environ* 2025, **978**, https://doi.org/10.1016/j.scitotenv.2025.179419.

56. Liu L, Zhang T, Wu Q, Xie L, Zhao Q, Zhang Y, *et al*.: **Highly sensitive detection of carbendazim in agricultural products using colorimetric and photothermal lateral flow immunoassay based on plasmonic gold nanostars**. *Talanta* 2025, **281**, https://doi.org/10.1016/j.talanta.2024.126891.

This study introduces a dual-mode LFIA employing gold nanostars (AuNSs) that enable both colorimetric and photothermal detection of carbendazim (CBD). The antibodies were passively adsorbed onto AuNSs, creating robust probes with LODs of 0.48 ng/mL (colorimetric) and 0.28 ng/mL (photothermal). The use of AuNSs expands the signal amplification capacity while maintaining simplicity in probe fabrication via physisorption. This work illustrates the growing utility of multimodal LFIAs and supports the continued relevance of non-covalent conjugation in high-sensitivity formats.

57. Wang Z, Zheng Z, Hu H, Zhou Q, Liu W, Li X, *et al*.: **A point-of-care selenium nanoparticle-based test for the combined detection of anti-SARS-CoV-2 IgM and IgG in human serum and blood**. *Lab Chip* 2020, **20**:4255–4261, https://doi.org/10.1039/D0LC00828A.

58. Wang L, Wu M, Ma J, Ma Z, Ren Y, Shao S, *et al*.: **Development of a point-of-care test based on selenium nanoparticles for heart-type fatty acid-binding proteins in human plasma and blood**. *Int J Nanomed* 2022, **17**:1273–1284, https://doi.org/10.2147/IJN.S359541.

59. Hu H, Tian Y, Yin X, Ren J, Su L, Xu J, *et al*.: **A lateral flow immunoassay based on chemisorbed probes in virtue of hydrogen bond receptors on the Bi2S3 NPs**. *Food Chem* 2023, **401**, 134133, https://doi.org/10.1016/J.FOODCHEM.2022.134133.

60. Zang X, Zhou Y, Li S, Shi G, Deng H, Zang X, *et al*.: **Latex microspheres lateral flow immunoassay with smartphone-based device for rapid detection of Cryptococcus**. *Talanta* 2025, **284**, 127254, https://doi.org/10.1016/J.TALANTA.2024.127254.

61. Tian Y, Chen L, Liu X, Chang Y, Xia R, Zhang J, *et al*.: **Colored cellulose nanoparticles with high stability and easily modified surface for accurate and sensitive multiplex lateral flow assay**. *ACS Nano* 2025, **19**:4704–4717, https://doi.org/10.1021/acsnano.4c15340.

62. Cardoso AR, Frasco MF, Serrano V, Fortunato E, Sales MGF: **Molecular imprinting on nanozymes for sensing applications**. *Biosensors* 2021, **11**:152, https://doi.org/10.3390/BIOS11050152. 2021;11:152.

63. Liu D, Ju C, Han C, Shi R, Chen X, Duan D, *et al*.: **Nanozyme chemiluminescence paper test for rapid and sensitive detection of SARS-CoV-2 antigen**. *Biosens Bioelectron* 2021, **173**, 112817, https://doi.org/10.1016/J.BIOS.2020.112817.

64. Sun B, Panferov V, Guo X, Xiong J, Zhang S, Qin L, *et al*.: **A novel triple-signal biosensor based on ZrFe-MOF@PtNPs for ultrasensitive aflatoxins detection**. *Biosens Bioelectron* 2025, **267**, 116797, https://doi.org/10.1016/j.bios.2024.116797.

65. Jiang H, Su H, Wu K, Dong Z, Li X, Nie L, *et al*.: **Multiplexed lateral flow immunoassay based on inner filter effect for mycotoxin detection in maize**. *Sensor Actuator B Chem* 2023, **374**, https://doi.org/10.1016/j.snb.2022.132793.

66. Dou L, Li Q, Wang Z, Shen J, Yu W: **AIEgens: next generation signaling source for immunoassays?** *ACS Sens* 2022, **7**:3243–3257, https://doi.org/10.1021/ACSSENSORS.2C02165.

67. Girmatsion M, Tang X, Zhang Q, Jiang J, Li P: **Phycocyanin-based rapid fluorometric immunoassay for the determination of aflatoxin B1, deoxynivalenol, and zearalenone in food and feed matrices**. *Food Control* 2024, **164**, 110585, https://doi.org/10.1016/J.FOODCONT.2024.110585.

68. Shi D, Yin Y, Li X, Yuan J: **Signal-boosted electrochemical lateral flow immunoassay for early point-of-care detection of liver cancer biomarker**. *ACS Sens* 2024, https://doi.org/10.1021/ACSSENSORS.4C01482.

69. Mateos H, Mallardi A, Serrano-Pertierra E, Blanco-López MC, Izzi M, Cioffi N, *et al*.: **Unusual gold nanoparticle-antibody interactions**. *JCIS Open* 2023, **11**, https://doi.org/10.1016/j.jciso.2023.100089.

70. Xue Y, Li X, Li H, Zhang W: **Quantifying thiol-gold interactions towards the efficient strength control**. *Nat Commun* 2014, **5**, https://doi.org/10.1038/ncomms5348.

71. Rashid U, Bro-Jørgensen W, Harilal K, Sreelakshmi P, Mondal RR, Chittari Pisharam V, *et al*.: **Chemistry of the Au-thiol interface through the lens of single-molecule flicker noise measurements**. *J Am Chem Soc* 2024, **146**:9063–9073, https://doi.org/10.1021/jacs.3c14079.

This publication offers a fundamental single-molecule-level study of the Au–S interface using flicker noise analysis in molecular junctions. It differentiates covalent Au–SR from weaker physisorbed Au–SRʹ′ interactions, demonstrating how structural variations in thiol ligands influence the stability and conductance of the bond. These insights clarify why covalent Au–S conjugation varies in robustness depending on the ligand's structure, offering mechanistic guidance for designing reliable LFIA bioconjugates.

72. Liang S, Chen S, Xu Z, Chen J, Lei H, Guan T: **A smartphone-based dual-modal lateral flow immunochromatographic assay for multiplex detection of illegal stimulant laxatives in slimming foods**. *Talanta* 2025, **285**, https://doi.org/10.1016/j.talanta.2024.127433.

73. Hristov DR, Pimentel AJ, Ujialele G, Hamad-Schifferli K: **The immunoprobe aggregation state is central to dipstick immunoassay performance**. *ACS Appl Mater Interfaces* 2020, **12**:34620–34629, https://doi.org/10.1021/acsami.0c08628.

74. Chen Y, Shen Y, Zhao Y, Zhu J, Wang H: **Rapid detection of zearalenone in cereals using La3+-doped upconversion nanoparticles-based immunochromatographic assay**. *Food Control* 2023, **153**, https://doi.org/10.1016/j.foodcont.2023.109904.

75. Wang Y, Liu P, Ye Y, Hammock BD, Zhang C: **An integrated approach to improve the assay performance of quantum dot-based lateral flow immunoassays by using silver deposition**. *Microchem J* 2023, **192**, https://doi.org/10.1016/j.microc.2023.108932.

76. Della Ventura B, Banchelli M, Funari R, Illiano A, De Angelis M, Taroni P, *et al*.: **Biosensor surface functionalization by a simple photochemical immobilization of antibodies: experimental characterization by mass spectrometry and surface enhanced Raman spectroscopy**. *Analyst* 2019, **144**: 6871–6880, https://doi.org/10.1039/c9an00443b.

77. Iarossi M, Schiattarella C, Rea I, De Stefano L, Fittipaldi R, Vecchione A, *et al*.: **Colorimetric immunosensor by aggregation of photochemically functionalized gold nanoparticles**. *ACS Omega* 2018, **3**:3805–3812, https://doi.org/10.1021/acsomega.8b00265.

78. Minopoli A, Della Ventura B, Lenyk B, Gentile F, Tanner JA, Offenhäusser A, *et al*.: **Ultrasensitive antibody-aptamer plasmonic biosensor for malaria biomarker detection in whole blood**. *Nat Commun* 2020, **11**, https://doi.org/10.1038/s41467-020-19755-0.

79. Minopoli A, Ventura B Della, Campanile R, Tanner JA, Offenhäusser A, Mayer D, *et al*.: **Randomly positioned gold nanoparticles as fluorescence enhancers in apta-immunosensor for malaria test**. *Microchim Acta* 2021, **88**:188, https://doi.org/10.1007/s00604-021-04746-9.

80. Li X, Wang J, Yang G, Fang X, Zhao L, Luo Z, *et al*.: **The development of aptamer-based gold nanoparticle lateral flow test strips for the detection of SARS-CoV-2 S proteins on the surface of cold-chain food packaging**. *Molecules* 2024, **29**, https://doi.org/10.3390/molecules29081776.

81. Dalirirad S, Han D, Steckl AJ: **Aptamer-based lateral flow biosensor for rapid detection of salivary cortisol**. *ACS Omega* 2020, **5**:32890–32898, https://doi.org/10.1021/acsomega.0c03223.

82. Tang Y, Yao L, Wang Y, Lin B, Yao Y, Chen L, *et al*.: **Signal-on lateral flow immunoassays for rapid detection of tetrodotoxin in pufferfish**. *J Hazard Mater* 2025, **486**, https://doi.org/10.1016/j.jhazmat.2024.136973.

83. Jiang CT, Chen KG, Liu A, Huang H, Fan YN, Zhao DK, *et al*.: **Immunomodulating nano-adaptors potentiate antibody-based cancer immunotherapy**. *Nat Commun* 2021, **12**, https://doi.org/10.1038/s41467-021-21497-6.

84. Guan Y, Zhang Y: **Boronic acid-containing hydrogels: synthesis and their applications**. *Chem Soc Rev* 2013, **42**: 8106–8121, https://doi.org/10.1039/c3cs60152h.

85. Michael Green N: **[5] Avidin and streptavidin**. *Methods Enzymol* 1990, **184**:51–67, https://doi.org/10.1016/0076-6879(90)84259-J.

86. Cui P, Li J, Chen B, Zhang Z, Ding Y, Liang H, *et al*.: **Preparation of peptides against immunocomplex of deltamethrin and application in noncompetitive lateral flow immunoassay**. *Food Chem* 2025, **471**, https://doi.org/10.1016/j.foodchem.2025.142757.

87. Cao Y, Chen Y, Zhang X, Zeng H, Cui L, He S: **Biotinylation-based lateral flow assays for pathogenic and total bacteria detection**. *Anal Chim Acta* 2025, **1338**, https://doi.org/10.1016/j.aca.2025.343607.

88. Zhou B, Ye Q, Li F, Xiang X, Shang Y, Wang C, *et al*.: **CRISPR/Cas12a based fluorescence-enhanced lateral flow biosensor for detection of Staphylococcus aureus**. *Sensor Actuator B Chem* 2022, **351**, https://doi.org/10.1016/j.snb.2021.130906.

89. Cai X, Ma F, Jiang J, Yang X, Zhang Z, Jian Z, *et al*.: **Fe-N-C single-atom nanozyme for ultrasensitive, on-site and multiplex detection of mycotoxins using lateral flow immunoassay**. *J Hazard Mater* 2023, **441**, 129853, https://doi.org/10.1016/j.jhazmat.2022.129853.

90. Shen J, Wang Y, Duan Z, Jin D, Shu Y, Hu X: **MOF scaffold for anchoring platinum-nickel nanoparticles with enhanced oxidase-like activity to improve lateral flow immunoassay diagnosis**. *Biosens Bioelectron* 2025, **273**, 117189, https://doi.org/10.1016/J.BIOS.2025.117189.

91. Wu N, Wei Y, Pan L, Yang X, Qi H, Gao Q, *et al*.: **Sensitive and rapid determination of heat shock protein 70 using lateral flow immunostrips and upconversion nanoparticle fluorescence probes**. *Analyst* 2022, **147**:3444–3450, https://doi.org/10.1039/D2AN00742H.

92. Wu KH, Huang WC, Shyu RH, Chang SC: **Silver nanoparticle-base lateral flow immunoassay for rapid detection of Staphylococcal enterotoxin B in milk and honey**. *J Inorg Biochem* 2020, **210**, 111163, https://doi.org/10.1016/J.JINORGBIO.2020.111163.

93. Bazsefidpar S, Serrano-Pertierra E, Gutiérrez G, Calvo AS, Matos M, Blanco-López MC: **Rapid and sensitive detection of E. coli O157:H7 by lateral flow immunoassay and silver enhancement**. *Microchim Acta* 2023, **190**, https://doi.org/10.1007/s00604-023-05834-8.